Recombinant expression and functional characterization of a novel toll interleukin receptor nucleotide-binding site leucine-rich repeat protein from *Arabidopsis thaliana*

by

Patience Chatukuta

Submitted in fulfilment of the requirements for the degree of Master of Science (MSc) in Biology in the Department of Biological Science, North-West University Mafikeng Campus, South Africa

Supervisor : Dr. Oziniel Ruzvidzo

November 2012

Declaration

I, Patience Chatukuta, declare that the thesis entitled "Recombinant expression and functional characterization of a novel toll interleukin receptor nucleotide-binding site leucine-rich-repeat protein from *Arabidopsis thaliana*" is my work and has not been submitted for any degree or examination at any other university and that all sources of my information have been quoted as indicated in the text and in the list of references.

Student: **Patience Chatukuta**

……. **Date:…….**

Supervisor: **Dr. O. Ruzvidzo**

……. **Date:…….....**

Dedication

This work is dedicated to a formidable pillar of strength, a great woman of God and an undisputed inspiration for my life, my mother, Irene Chatukuta.

Acknowledgements

According to the Book of Daniel Chapter 11, Verse 11, the Holy Bible sums it up thus "…but the people that do know their God shall be strong, and do exploits." Therefore, first and foremost, all glory be to God for His enabling power.

I sincerely appreciate the unending patience of my supervisor, Doctor Ruzvidzo, who has an amazing ability to put up with a load of baloney and still conduct himself as the best supervisor in the world.

My co-supervisor, Doctor Kwezi, was my 'go-to' person with regard to molecular biology techniques, and the skills I have gained from my interaction with him are invaluable, and notably, marketable.

Professor Christoph Gehring laid the foundation for this research. I am honoured to have added a few bricks to this great building that his research spawned.

I extend my gratitude to all academic staff, technicians and postgraduate students of the Biological Sciences Department who were always willing and ready to help.

This research would not have been possible without funding from the North-West University Mafikeng Campus, the National Research Foundation, and the Organisation for Women Scientists from Developing Countries in conjunction with the Swedish International Development Agency. I thank the relevant staff who facilitated the awards and transfers of funds.

The members of my church in Mmabatho became my family away from home. May God bless them abundantly.

Finally, I thank my family for the moral support and the continuous ribbing about me being a 'biotech geek'. I welcome the love, and the jokes, always.

Ndatenda hangu.

Definitions of Terms

Adenylate cyclases (ACs): Enzymes capable of converting adenine-5′-triphosphate (ATP) to cyclic 3′, 5′-adenosine monophosphate (cAMP).

***Arabidopsis thaliana*:** A small flowering plant that is widely used as a model research organism in plant biology.

Enzyme immunoassay: An antibody-based diagnostic technique used in molecular biology for the qualitative and quantitative detection of specific biological molecules.

Guanylate cyclases (GCs): Enzymes capable of converting guanine-5′-triphosphate (ATP) to cyclic 3′, 5′-guanosine monophosphate (cGMP).

Primers: Short synthetic nucleic acid sequences capable of forming base pairs with complementary template RNA/DNA strand and facilitating its specific amplification.

Reverse transcription polymerase chain reaction (RT-PCR): A molecular method used to amplify a short RNA segment into a DNA product termed copy DNA (cDNA) using an RNA-dependent DNA polymerase enzyme.

Second messenger: A biological molecule capable transmitting external cellular signals within the cell for the development of appropriate cellular responses through regulated gene expression and metabolic events.

Sodium dodecyl sulphate polyacrylamide gel electrophoresis (SDS-PAGE): A technique used in molecular biology to separate different protein molecules according to their sizes and migration levels in a polyacrylamide gel system subjected to a strong electrical field.

List of Abbreviations

2YT – Double-strength yeast-tryptone

3D- Three dimensional

ADP - Adenosine diphosphate

AKAP – A-kinase anchoring protein

Amp^R – Ampicillin resistance

ATP - Adenosine-5′-triphosphate

ATPase – Adenosine triphosphatase

BLAST – Basic local alignment search tool

BN – Blue native

bp – Base pairs

cAMP - Cyclic adenosine monophosphate

CARD – Mammalian caspase recruitment domain

CATERPILLAR - Caspase activation and recruitment domains [CARD], transcription enhancer, R [purine]-binding, pyrin, many leucine repeats family

CC – Coiled coil

cDNA – Complementary DNA

CTAB - Hexadecyltrimethyl-ammonium bromide

C-terminus – Carboxy terminus

DNA - Deoxyribonucleic acid

dNTP - Deoxyribonucleotide triphosphate

ECS – Endocytosis cell signalling domain

EDTA - Ethylenediaminetetraacetic acid

EGTA - Ethylene glycol tetraacetic acid

EIA – Enzyme immunoassay

ELISA – Enzyme-linked immunosorbent assay

eLRR – Extracytoplasmic leucine-rich repeat

EPAC – Exchange protein directly activated by cAMP

GC – Guanylate cyclase

GTE – Glucose Tris EDTA

GTP - Guanosine-5′-triphosphate

His – Histidine

HM1 – *Helminthosporium carbonum* toxin reductase enzyme

HR – Hypersensitive response

IBMX - 3-isobutyl-1-methyl xanthine

IPTG – Isopropyl-β-D-1-thiogalactopyranoside

kb - Kilobases

kDa - Kilodaltons

LB – Luria Bertani

LRR - Leucine-rich repeat

MS – Murashige and Skoog

NACHT - NAIP, CIITA, HET-E and TP1 NTPase domain

NB – Nucleotide binding

NB-ARC - NB, ARC1, and ARC2 ATPase domain

NBS - Nucleotide binding site

Ni–NTA – Nickel nitriloacetic acid

NLPp$_p$ – Necrosis and ethylene-inducing peptide1-like protein from *Phytophthora sojae*

NLS – Nuclear localisation signal

Nod – Nucleotide-binding oligomerisation

NSB – Non-specific binding

PAGE – Polyacrylamide gel electrophoresis

PAMP - Pathogen-associated molecular patterns

PCR – Polymerase chain reaction

PEST – Pro-Gly-Ser-Thr protein degradation domain

PKA – Protein kinase A

PMSF – Phenylmethylsulphonyl fluoride

PNP – Plant natriuretic peptide

PPR - Pathogen recognition receptors

PTI – Pathogen-associated molecular pattern-triggered immunity

R – Resistance

RGA – Resistance gene analog

RNA - Ribonucleic acid

RNase - Ribonuclease

rpm – Revolutions per minute

RT-PCR – Reverse transcriptase polymerase chain reaction

SAR – Systemic acquired response

SDS – Sodium dodecyl sulphate

SOB – Super optimal broth

SOC – Super optimal broth with catabolite repression

SSTE - Sodium dodecyl sulphate-Tris-HCl-EDTA

STAND – Signal transduction ATPases with numerous domains

TAIR – The Arabidopsis Information Resource

Taq - *Thermus aquaticus*

TBS – Tris-buffered saline slution

TEMED – Tetramethylethylenediamine

TIR - Toll/interleukin-1 receptor

TrD – Transmembrane domain

LISTS OF FIGURES AND TABLES

FIGURE **PAGE**

TABLES

PAGE

TABLE OF CONTENTS

Abstract

The presence of adenylate cyclases in higher plants has generally been questioned. A BLAST search of the *Arabidopsis* genome using a 14-amino acid motif with specificity for ATP binding bioinformatically identified the toll interleukin-like receptor nucleotide binding site leucine rich repeat (TIR-NBS-LRR) protein encoded by the At3g04220 gene from *Arabidopsis thaliana* to have a putative adenylate cyclase catalytic centre. To test whether TIR-NBS-LRR possesses adenylate cyclase activity, total mRNA was extracted from the leaf material of 6-week old *A. thaliana* plants and used as template for complementary DNA synthesis and amplification of a 114 amino acid-long adenylate cyclase catalytic domain fragment of the At3g04220 gene using Reverse Transcriptase Polymerase Chain Reaction in conjunction with sequence-specific primers. The amplified fragment was then cloned into a pCR®T7/NT-TOPO® vector and the recombinant vector was transformed into the expression host, *Escherichia coli* BL21 (DE3) pLysS. Positive transformants were determined using Sodium Dodecyl Sulphate Polyacrylamide Gel Electrophoresis; and confirmed by sequence-specific colony PCR and restriction double digestion. The His-tagged recombinant protein was over-expressed following induction with isopropyl-β-D-1-thiogalactopyranoside and purified using a nickel affinity gel system. The endogenous and *in vitro* adenylate cyclase activities of the recombinant TIR-NBS-LRR were then tested via a cAMP-specific enzyme immunoassaying system and the *in vivo* adenylate cyclase activity was tested through a complementation test using the *Escherichia coli cya*A SP850 mutant. The results of all these three assays indicated that the TIR-NBS-LRR protein encoded by the At3g04220 gene from *A. thaliana* possessed endogenous, *in vitro* and *in vivo* adenylate cyclase activities, and thus, confirmed TIR-NBS-LRR as a higher plant adenylate cyclase with a possible cAMP-mediated signaling system.

CHAPTER 1

GENERAL INTRODUCTION AND LITERATURE REVIEW

1.1 INTRODUCTION

A major determinant of plant growth is how plants respond to stressful conditions brought on by biotic and abiotic stresses such as pathogenic infections, drought and salinity. In the arid and semi-arid areas of Southern Africa, these stresses continue to contribute towards the problem of crop loss (Denby and Gehring, 2005). This prevailing situation, in the face of rapidly mutating pathogens and climate change, will inevitably lead to increased demand for food and therefore, a consequent rise in the cost of limited resources. Food security is, therefore, heavily dependent on the development of crop plants with increased resistance to biotic and abiotic environmental factors (Atkinson and Erwin, 2012). Recent advances in the areas of plant biochemistry, plant physiology and plant biotechnology have simplified the process of over-expression and lateral transfer of plant genes which are capable of increasing tolerance of plants to stress factors. The approach of plant biotechnology in this regard has been to focus on plant molecules which are systemically known to be involved in the maintenance of homeostasis and response to stress (Hussain *et al.,* 2010). This study has focused on the characterisation of one such molecule, the toll interleukin-like receptor nucleotide binding site leucine-rich repeat (TIR-NBS-LRR) protein from *Arabidopsis thaliana*. Recombinant expression and molecular characterisation of TIR-NBS-LRR was conducted with the aim of possibly applying the understanding of its functionality to the Southern African agricultural context for the improvement of both crop yield and food security.

TIR-NBS-LRR was bioinformatically annotated as a putative higher plant adenylate cyclase (Gehring, 2010) and was, therefore, a target protein for this study. This is because adenylate cyclases are enzymes capable of generating the second messenger cAMP which is commonly

involved in several plant cellular signal transduction processes, including those of resistance to stressful conditions.

1.1.1 Problem Statement

TIR-NBS-LRR has been implicated in disease tolerance (Gassmann *et al.,* 1999) and salinity tolerance (Qutob *et al*., 2006). However, no study has experimentally demonstrated TIR-NBS-LRR's ability to generate cAMP although cAMP is known to participate as a second messenger in all stress tolerance processes where TIR-NBS-LRR is actively involved. In addition, apart from the *Zea mays* pollen protein (Moutinho *et al*., 2001) which is the only protein so far to have been characterised as an adenylate cyclase, no other higher plant protein has ever been characterised. As such, a need was identified to experimentally explore the putative adenylate cyclase catalytic activity of the recently identified and annotated TIR-NBS-LRR protein from *A. thaliana* (Gehring, 2010) and possibly determine its functional role in stress response and adaptation mechanisms..

1.1.2 Aim of the Research Study

This study sought to ascertain whether TIR-NBS-LRR is capable of generating cAMP from ATP, and if so, to then denote it as a possible biomolecule with possible involvement in plant stress response and adaptation mechanisms. Additionally, this study also sought to establish whether higher plants do possess other adenylate cyclases apart from the known *Zea mays* pollen protein.

1.1.3 Objectives of the Research Study

Specific objectives were set to be met in addressing the research question as follows:

1. Bioinformatic analysis of the At3g04200 gene.
2. Isolation and cloning of the annotated Arabidopsis TIR-NBS-LRR gene (At3g04220) into stable and viable heterologous prokaryotic expression systems.
3. Optimisation of strategies for the expression and purification regimes of the recombinant TIR-NBS-LRR protein.
4. Determination of the endogenous biological activity of the recombinant TIR-NBS-LRR protein in a bacterial system.
5. Further characterisation of the enzymatic activities of this TIR-NBS-LRR protein *in vitro* and *in vivo.*

1.1.4 Significance of the Research Study

This study is significant in that the functional characterisation of the annotated TIR-NBS-LRR gene will contribute towards a better understanding of the general mechanisms by which plants respond and adapt to stressful conditions. The improved scientific knowledge regarding genes responsible for stress response and adaptation will contribute towards the integrated management of both biotic and abiotic stressful conditions of agronomically important crops in South Africa. In addition, this research will add to the academic literature on higher plant adenylate cyclases, which is a field that has scant literature in comparison to microbial and mammalian adenylate cyclases.

1.2 LITERATURE REVIEW

1.2.1 PLANT DISEASE RESISTANCE

Plants have developed numerous mechanisms for counteracting pathogen attacks. The importance of this capability is underscored by the existence of various plant disease resistance (*R*) genes and of germline-encoded proteins known as pathogen recognition receptors (PRRs) which recognise numerous conserved pathogen-associated molecular patterns (PAMPs) (Rairdan and Moffett, 2007). In plants, the arsenal of inducible defense responses comprises the hypersensitive response (HR), tissue reinforcement and antibody production. These local responses can trigger the systemic acquired response (SAR), a long-lasting systemic response that primes the plant for resistance against a broad spectrum of pathogens. Tight genetic control is exerted over plant defenses which are activated only if the plant detects a prospective invader. Hence, plants autonomously maintain constant vigilance against pathogens by expressing large arrays of *R* genes (McDowell and Woffenden, 2003).

Plant disease resistance genes can both be variable within and between populations, and specific *R* genes are often present only in certain plant cultivars or accessions (Rairdan and Moffett, 2007). The diverse evolutionary patterns in *R* genes are possibly a result of adaptation, which allows plants to cope with different types of pathogens (Chen *et al.,* 2009). When induced in a timely manner, *R* genes can efficiently halt pathogen growth with minimal collateral damage to the plant. This makes *R* gene-mediated resistance attractive to farmers since it requires no external input and has no adverse environmental effects.

Based on amino acid motif organisation and membrane spanning domains, *R* genes can be broadly divided into eight groups as is shown below and in Figure 1.1. These code for:

- Cytoplasmic NBS-LRR proteins with an N-terminal toll-interleukin receptor domain (TIR-NBS-LRR).
- Cytoplasmic NBS-LRR proteins with an N-terminal coiled-coil domain (CC-NBS-LRR).
- Extracytoplasmic LRRs attached to a transmembrane domain (eLRR-TrD).
- Extracytoplasmic LRR-TrDs with an intracellular serine-threonine kinase domain (eLRR-TrD-KIN).
- Putative extracellular LRRs with a PEST domain and short proteins motifs (LRR-TrD-PEST-ECS).
- Proteins with a membrane domain fused to a putative coiled-coil domain (TrD-CC).
- TIR-NBS-LRR proteins with a putative nuclear localisation signal and a WRKY domain (TIR-NBS-LRR-NLS-WRKY).
- Enzymatic R proteins which contain neither LRR nor NBS groups (Gururani *et al.*, 2012).

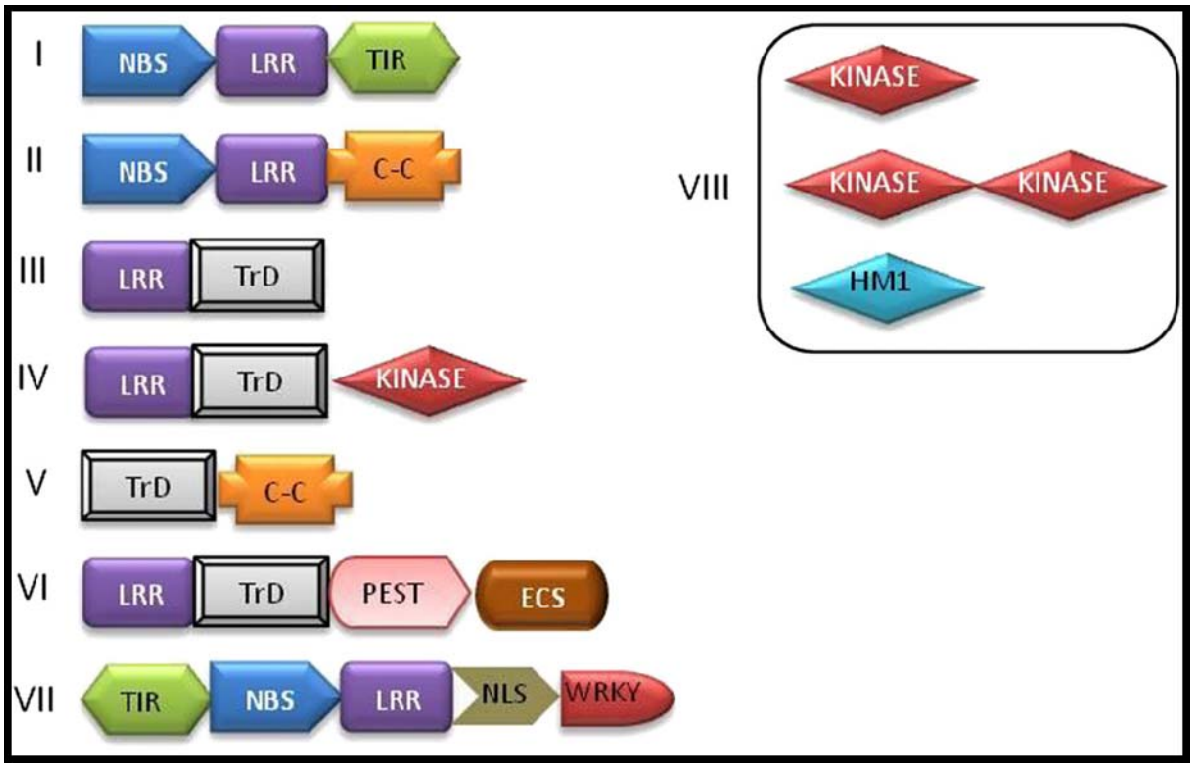

Figure 1.1: Arrangement of functional domains of major classes of *R* genes. LRR – Leucine-rich repeat, NBS – Nucleotide-binding site, TIR – Toll-interleukin receptor, CC – Coiled-coil, TrD – Transmembrane domain, PEST – Pro-Gly-Ser-Thr protein degradation domain, ECS – Endocytosis cell signalling domain, NLS – Nuclear localisation signal, WRKY – Amino acid domain, HM1 – *Helminthosporium carbonum* toxin reductase enzyme (Adapted from Gururani *et al*., 2012)

R genes confer resistance to a wide variety of pathogens including bacteria, viruses, oomycetes, fungi, nematodes and insects (Gururani *et al*., 2012; Rairdan and Moffett, 2007). Functionally characterised *R* genes have been implicated in bacterial, fungal, oomycete, nematode, viral, insect and broad range resistance in a variety of grain crops, root crops, vegetables and legumes (Gururani *et al.,* 2012).

1.2.2 THE NBS-LRR PROTEINS

The genes encoding nucleotide binding site leucine-rich repeat (NBS-LRR) proteins are the most common of the *R* genes, making up 75 percent of *R* genes (Chen *et al.,* 2009). They are related to the mammalian caspase recruitment domain (CARD)/nucleotide-binding oligomerisation domain (Nod) family, which also functions in innate immunity (Belkhadir *et al.*, 2004). Although the NBS-LRR proteins reside within the cytoplasm, they are mobile and can translocate into the nucleus, chloroplast or mitochondria; or be located across the plasma membrane (Tor *et al.,* 2009). They function as macromolecular complexes (Mc Hale *et al.*, 2006) consisting of four domains; the amino terminus, the NBS domain, the LRR domain and the carboxyl terminus. The NBS-LRR family of proteins may further be divided into two subfamilies based on the presence of an amino-terminal toll and human interleukin receptor (TIR) domain or the absence of the TIR structural domain (non-TIR).

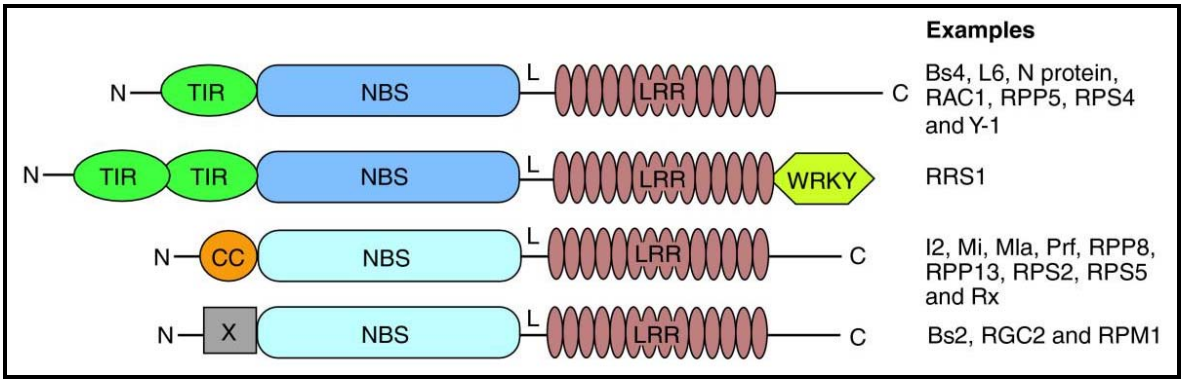

Figure 1.2: Types of NBS-LRR proteins. Examples of proteins with each configuration shown on the right. Bs4, I2, Mi, and Prf are from tomato; L6 from flax; N from tobacco; RAC1, RPP5, RPS4, RRS1, RPP8, RPP13, RPS2, RPS5, and RPM1 from Arabidopsis; Y-1 and Rx from potato; Mla from barley; RGC2 from lettuce; Bs2 from pepper. N, amino terminus; TIR, Toll/interleukin-1 receptor-like domain; CC, coiled-coil domain; X, domain without obvious CC motif; NBS, nucleotide binding site; L, linker; LRR, leucine-rich repeat domain; WRKY, zinc-finger transcription factor-related domain containing the WRKY sequence; C, carboxyl terminus (Adapted from McHale *et al*., 2006).

Non-TIR-NBS-LRR proteins commonly have a coiled-coil (CC) motif in the N-terminal of their structural domains (Chen *et al*., 2009; Eitas and Dangl, 2010) although some may also have a domain without an obvious CC motif at the amino terminal or a WRKY sequence at the carboxy terminal as shown in Figure 1.2 (McHale *et al.,* 2006). The NBS-LRR class of *R* genes has been identified in various plant species, in monocots as well as dicots. Although the two subclasses of NBS-LRR genes are present in gymnosperm and dicot genomes, TIR-NBS-LRR-encoding genes are completely absent from monocot genomes (Geffroy *et al.,* 2008).

Although plant genomes contain genes which code for hundreds of NBS-LRR proteins, relatively few have been functionally characterised (Tameling and Joosten, 2007). The use of highly conserved motifs, and genomic and EST projects to generate numerous resistance gene analogs (RGAs) that span at least part of the NBS domain have resulted in the isolation of RGAs from a wide variety of plants (Cannon *et al*., 2002), and these RGAs have then been used as

probes for genetic screening (Pan *et al*., 2000; Que *et al.,* 2009). Utilisation of conserved motifs as a basis for PCR has resulted in cloning of over 50 NBS-LRR proteins with known recognition specificities due to the highly conserved nature of the NBS domains and the core residues of the LRR domains, even among distantly related NBS-LRR-encoding genes (McDowell and Woffenden, 2003; Radwan *et al*., 2008). However, NBS-LRR encoding genes often contain hundreds of family members in plant genomes (Radwan *et al*., 2008). Genome sequencing has revealed a much larger degree of diversity, including 150 NBS-LRR encoding genes in the Arabidopsis genome (Jones, 2001), approximately 400 in poplar and over 500 in rice (Rairdan and Moffett, 2007).

Although these genes are one of the most prevalent classes in plant genomes, little is known of their function. In addition, the functions of many proteins and other molecules which interact with *R* genes during defense mechanisms are largely unknown (Gachomo *et al.,* 2003). Indications from the sequences of *R* gene motifs are that they are involved at the commencement of signalling pathways. NBS-LRR-encoding genes were once thought to play a role only in disease or pest resistance and innate immunity (Michelmore, 2000), but subsequent studies have shown that they are also involved in signalling functions other than innate immunity, such as drought-tolerance, shade avoidance, photomorphogenesis, and development (Tameling and Joosten, 2006).

Some NBS-LRRs, such as the tomato *NRC1* and tobacco *NRG1*, have been identified as innate immunity signalling components downstream of immune receptors. While the *adr1* mutant of Arabidopsis shows a constitutive defence phenotype related to enhanced resistance to biotrophic pathogens, it also shows a striking and markedly enhanced drought tolerance (Grant *et al*., 2003).

In sunflower, absence of *PLFOR48* activity has been shown to cause severe developmental abnormalities such as stunted growth and reduced apical dominance. An Arabidopsis NBS-LRR gene for constitutive shade avoidance (CSA1) has been identified via the mutagenesis approach (Tameling and Joosten, 2007).

Further to the rapid advances in analytical tools and capabilities in the field of molecular biology, there has been a shift away from identification and manipulation of individual genes to global characterisation of resistance phenotypes. It has been suggested that characterisation of the genes encoding NBS-LRR proteins will provide clues as to the variety of functions performed by the NBS-LRR genes (Michelmore, 2000).

1.2.2.1 Prevailing Models for the Molecular Basis of NBS-LRR Defense Systems In Plants

NBS-LRR sequences are often tightly linked at complex loci. In the Arabidopsis genome, for example, 73.2 percent of the NBS-LRR sequences are located in clusters of genes. There is remarkable variation in the frequency of recombination between clustered genes, even within a single cluster. The clustered organisation is supposed to favour sequence exchanges, such as unequal crossing over and/or gene conversion events, which can give rise, in some cases, to new, non-parental *R* specificities (Geffroy *et al*., 2008; Gururani *et al*., 2012).

It has been shown that the vast majority of NBS-LRR proteins recognise proteins extracellularly, intracellularly, upon synthesis within the cell, or upon delivery into the plant cytoplasm (Geffroy *et al*., 2008). NBS-LRR proteins recognise effectors, which are proteins, deployed by pathogens to suppress pathogen associated molecular pattern triggered immunity (PTI) (Eitas and Dangl,

2010). In effect, NBS-LRR proteins do not respond to PAMPs or small antigens, but generally recognise functionally and structurally intact proteins. The defense response triggered by NBS-LRR proteins is characterised by rapid calcium and ion fluxes, an extracellular oxidative burst, transcriptional re-programming within and around the infection sites, and in most cases, a localised programmed cell death termed the hypersensitive response (HR); thus leading to a halt in biotrophic pathogen growth (Belkhadir *et al*., 2004; Rairdan and Moffett, 2007).

Several well-tailored genetic approaches have tried and failed to reveal the mechanistic and physiological basis of NBS-LRR action (Belkhadir *et al.,* 2004). Staskawitz (2001) recognised the identification of the molecular basis of plant disease resistance specificity as "today's 'Holy Grail'" in the field of molecular plant pathology. Initially, the **gene-for-gene model** of NBS-LRRs in plant disease resistance was postulated following research characterising the interaction between the fungal pathogen flax rust (*Melampsora lini*) and flax (*Linum usitatissimum*) (Flor, 1971; Rairdan and Moffett, 2007;). This model contends that the outcome of pathogen-plant interaction is determined by whether a plant resistance gene (*R*) coincides with a corresponding pathogen avirulence gene (*avr*) (Eitas and Dangl, 2010). The resistance response is appended with the hypersensitive response (HR) caused by a signalling cascade triggered by recognition of an effector by the NBS-LRR-encoding gene or by recognition of plant defense response elicitor by a specific receptor (Gururani *et al.,* 2012). However, experimental data to support this model are rare (Belkhadir *et al*., 2004).

As a way of framing indirect recognition, the **'guard hypothesis'** has been postulated as an alternative to the gene-for-gene model for pathogen-plant interaction. This hypothesis exists in the context of the interplay between pathogen virulence factors and host proteins (Rairdan and

Moffett, 2007). It has been shown that the avirulence proteins which contribute to disease are actually required for maximal virulence on susceptible hosts that lack the corresponding *NBS-LRR* gene. It is therefore plausible that NBS-LRR proteins have evolved to recognise the functions of pathogen virulence factors as they modify host cellular targets (Belkhadir *et al.*, 2004). The most convincing evidence to date for the guard hypothesis has been found in *A. thaliana* where a cellular protein was identified as being essential for the resistance to *Pseudomonas syringae* pv. tomato (Gururani *et al*., 2012).

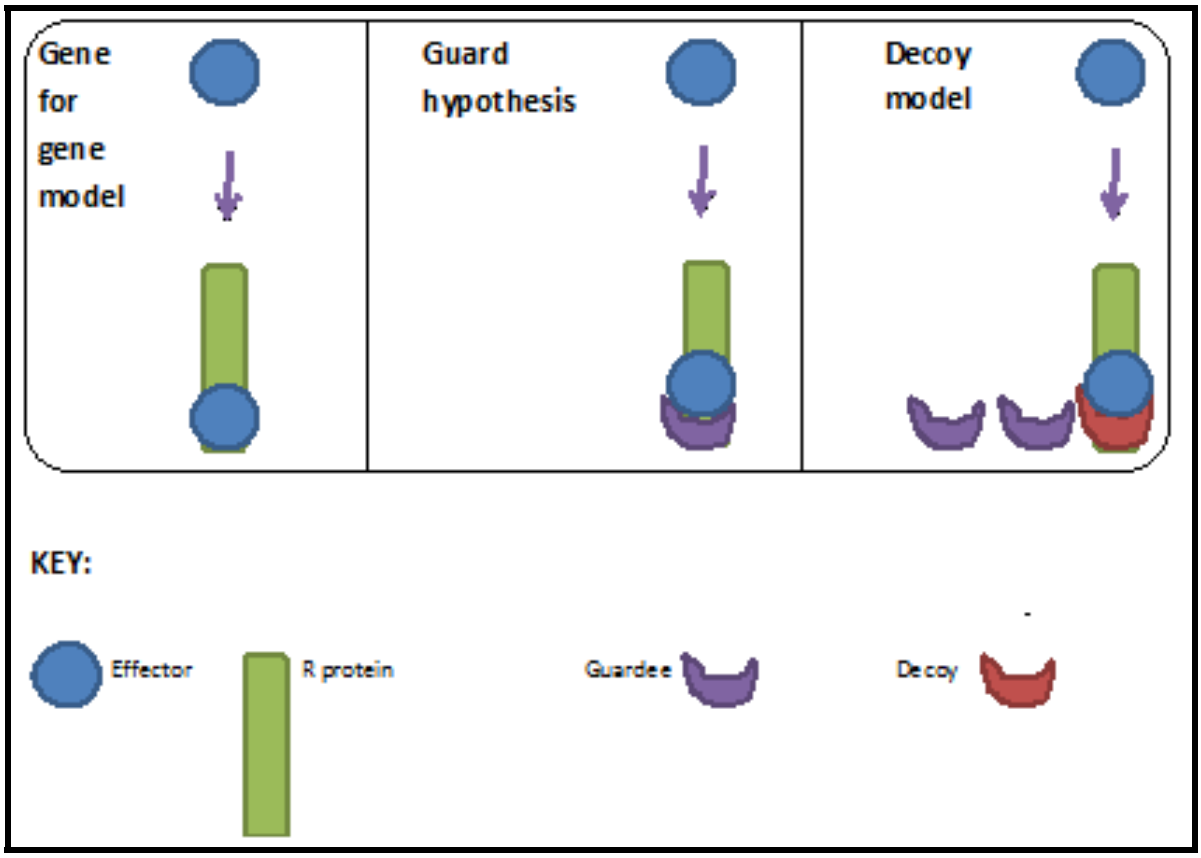

Figure 1.3: Comparison of the models of disease resistance role of NBS-LRRs. The gene for gene model is illustrated by the effector directly attaching to the R protein. The guard hypothesis is illustrated by the attachment of both the effector and the 'guardee' proteins directly to the R protein. The decoy model is illustrated by the attachment of both the effector and the decoy proteins to the R protein, leaving the 'guardee' unattached.

However, new data on indirectly recognised effectors is inconsistent with the guard hypothesis. This situation has given rise to the **'decoy model'** (Figure 1.3) which is consistent with the relevant data. The decoy is the host protein which specialises in perception of the effector by the NBS-LRR protein but itself has no function either in development of disease and resistance. Hence, the decoy mimics effector targets to trap the pathogen into a recognition event without contributing pathogen fitness in the absence of its cognate R protein (Van der Hoorn and Kamoun, 2008).

1.2.2.2 Physiological Roles of the NBS and LRR Domains

Recently, it has been suggested that NBS-LRR protein changes in intramolecular interactions and conformation associated with nucleotide exchange by the NBS domain are induced by effector recognition, thus exposing an N-terminal signalling domain to activate downstream defense response (Bernoux *et al.,* 2011). Several studies indicate that NBS-LRR proteins are subject to constitutive negative regulation. The proteins' domains may function as an on and off switch in intramolecular interactions, where the CC or the TIR domain are critical for this process (Belkhadir *et al*., 2004).

<u>The amino terminus</u>

The amino-termini of the TIR-NBS-LRR proteins are thought to be involved in protein-protein interactions, possibly with the proteins being guarded from pathogens or with downstream signalling components (McHale *et al*., 2006).

The NBS domain

The Nucleotide Binding Site (NBS) domain is also known as the NOD, NACHT, CATERPILLAR or NB-ARC domain. It consists of motifs characteristic of the 'signal transduction ATPases with numerous domains' (STAND) family of ATPases which are regulated by nucleotide binding, nucleotide hydrolysis and intramolecular domain interactions (Eitas and Dangl, 2010). The STAND ATPases often combine N-terminal effector domains followed by the ATPase domain and a C-terminus composed of superstructure-forming repeats such as LRR or WD-40 domains. They function as molecular switches in disease signalling pathways.

The N-terminal sub-domain of the NBS domain contains consensus kinase 1a (P-loop), kinase 2 and kinase 3a motifs common to a large variety of nucleotide-binding proteins, that is, the NB subdomain (Moffett *et al.,* 2002).

The NBS domain has been described as a region spanning 300 amino acids containing several motifs that are strictly ordered (Lozano *et al.,* 2012). The conserved sequence consensus G-x-x-G-x-G-K-T-T (where x is any amino acid) has been found to be present in almost all NBS domains of NBS-LRR-type resistance genes (Pan *et al.,* 2000) and is contiguous with a C-terminal extension designated the ARC domain due to its conservation in Apaf-1, R proteins and CED4 in plants (Rairdan and Moffett, 2007; Tameling and Joosten, 2007).

Initially, the NBS domain was believed to alter the activation state of the molecule enabling signal transduction, but this molecular model has been derided for being too simplistic with the intramolecular interactions occurring between domains (Sadras and Calderini, 2009). *In vitro*

binding studies suggest that the NBS domain provides a molecular switch by alternating between two different states: the resting ADP-bound state and the active ATP-bound state (Xiao, 2008).

The NBS sequence motif is found in many ATP- and GTP-binding proteins (Pan *et al.,* 2000), and it functions in nucleotide binding and hydrolysis (Belkhadir *et al*., 2004) which is thought to result in conformational changes that regulate downstream signalling (McHale *et al.,* 2006).). The NB-ARC domain from the I2 resistance protein and Apaf-1 exhibits ATPase activity *in vitro*, thus implying that an energy-dependent conformational change in NBS-LRR proteins is crucial for their activity (Swiderski *et al*., 2009). The domain has also been known to mediate ligand-induced homo-oligomerization of mammalian NBS proteins (Ade *et al.,* 2007).

The LRR domain

The Leucine-Rich Repeat (LRR) domain comprises of a core of about 26 amino acids containing the Leu-xx-Leu-xx-Leu-x-Leu-xx-Cys/Asn-xx motif (where x is any amino acid), which forms a β-sheet. LRRs consist of 2 to 45 motifs that generally fold into an arc or horseshoe shape (Enkbayar *et al*., 2004). The concave face and the adjacent loops are the most common protein interaction surfaces on LRR proteins. The 3D structures of some LRR protein-ligand complexes show that the concave surface of the LRR domain is ideal for interaction with α-helices, thus supporting earlier conclusions that the elongated and curved LRR structure provides an ideal framework for achieving diverse protein-protein interactions (Kobe and Kajava, 2001). Molecular modeling suggests that the conserved pattern Leu-xx-Leu-x-Leu, which is shorter than the previously proposed Leu-xx-Leu-x-Leu-xx-Asn/Cys-x-Leu, is sufficient to impart the characteristic horseshoe curvature to proteins with 20- to 30-residue repeats (Kajava and Kobe, 2002).

LRRs occur in proteins ranging from viruses to eukaryotes, and appear to provide a structural framework for the formation of protein-protein interactions (Kobe and Kajava, 2001; Enkbayar *et al.,* 2004). Proteins containing LRRs include tyrosine kinase receptors, cell-adhesion molecules, virulence factors, and extracellular matrix-binding glycoproteins, and are involved in a variety of biological processes, including signal transduction, cell adhesion, DNA repair, recombination, transcription, RNA processing, disease resistance, apoptosis and the immune response (Rothberg *et al.,* 1990).

The LRR domain is involved in determining the recognition specificity of several disease resistance proteins (McHale *et al*., 2006) by modulating activation and recognition of pathogenic elicitors via mediation of protein-protein and protein-ligand interactions (Belkhadir *et al.,* 2004; Swiderski *et al.,* 2009). Genetic and molecular analysis has shown that recognition specificity resides within the LRR domain, which tends to be highly variable and subject to diversifying selection (Rairdan and Moffett, 2007). Significantly, LRRs with adenylate cyclase activity have been reported (Suzuki *et al*., 1990).

The carboxy terminus

The carboxy termini of the TIR-NBS-LRR proteins often have 240-380 amino acids, equalling the size of the LRR domain (McHale *et al.,* 2006).

1.2.3 TIR-NBS-LRR PROTEINS

Toll interleukin-like receptor nucleotide-binding site leucine-rich repeat (TIR-NBS-LRR) sequences with characteristic RNBS-A motifs have been found in the grass family (Poaceae), bryophytes, gymnosperms and eudicots; and they play a physiological role in disease resistance in plants. The TIR-NBS-LRR subfamily contains atypical domain combination, with many occurring within one genomic cluster. This analysis shows that the gene family is not only important functionally and agronomically, but also plays a structural role in the genome (Ameline-Torregrosa *et al.,* 2008).

TIR-NBS-LRR sequences have been successfully amplified from dicot and gymnosperm DNA but not from monocot DNA. Hence, the presence of TIR-NBS-LRR sequences has been well-established in basal angiosperms but rarely so in monocots or magnoliids (Tarr and Alexander, 2009). Within the Arabidopsis genome, the TIR-NBS-LRR-encoding genes make up approximately 60 percent of all NBS-LRR-encoding genes (Jones, 2001).

An investigation into the relationships between gene family and plant lineage diversification in the NBS-LRR family showed that, in contrast to the non-TIR branch, the TIR-NBS-LRR family is more homogeneous, suggesting either later divergence or more extensive structural constraints (Cannon *et al*., 2002).

TIR-NBS-LRR proteins are NBS-LRR proteins with an N-terminal domain with significant similarity to the *Drosophila* Toll or human interleukin-1 receptor-like (TIR) region (Pan *et al.,* 2000; Rairdan and Moffett, 2007). In *Drosophila*, the Toll receptor is essential for establishing dorsoventral pattern in embryos and inducing the immune response in the adult fly (Pan *et al.,*

2000). The induction of pro-inflammatory cytokines via a transcription factor in the mammalian Interleukin-1R pathway has striking resemblance to the signal transduction cascade downstream of Toll (Gassmann *et al*., 1999). Several human homologues of the Toll (h-Toll) protein have been isolated and shown to signal adaptive immunity and mediate lipopolysaccharide-induced cellular signalling (Pan *et al*., 2000).

TIR-NBS-LRR proteins detect pathogen-associated proteins, most often, the effector molecules of pathogens responsible for virulence. Association with either a modified host protein or a pathogen protein leads to conformational changes in the amino-terminal and LRR domains of the TIR-NBS-LRR proteins and such conformational alterations then promote the exchange of ADP for ATP by the NBS domain, activating 'downstream signalling', leading to pathogen resistance (DeYoung and Innes, 2006).

Gassmann and colleagues (1999) characterised the Arabidopsis *RPS4* gene and established a role for TIR-NBS-LRR genes in specifying resistance to a bacterial pathogen. By analysing the TIR domain of the RPS4 protein by site-directed mutagenesis and characterisation of gain-of-function substitutions, Swiderski and colleagues (2009) then revealed that the TIR domain functions in apoptosis and that the NBS domain is not necessary for this function. Expression of truncated derivatives of TIR-NBS-LRR proteins showed that a TIR domain with a short C-terminal fragment directly following it is sufficient to cause cell death. Because the construct that solely expresses the TIR domain did not produce a detectable amount of protein, it is, however, unclear whether the TIR domain alone is sufficient to signal cell death. Hence, it has been suggested that a part of the sequence between the TIR domain and the NBS motif is also important for signalling with the TIR domain itself (Swiderski *et al*., 2009).

In addition to pathogen detection, it has also been suggested that the TIR domain may also function to direct expression of genes involved in defence responses (Burch-Smith and Dinesh-Kumar, 2007). The TIR domain is believed to propagate the perception signal (Gachomo *et al.*, 2003) and is dependent on a functional EDS1 allele to provide pathogen resistance (Gassmann, 1999; Swiderski *et al.,* 2009).

The *N* and the *L6* genes were the first genes shown to belong to the *TIR-NBS-LRR* subfamily, encoding resistance to viral and fungal pathogens respectively. The *RPP5* gene from Arabidopsis was also one of the earliest *R* genes to be cloned in the 1990's and it was shown to encode resistance to oomycete pathogens (Bent, 1996; Gassmann *et al.,* 1999).

TIR-NBS-LRR-encoding genes were once thought to play a role only in disease or pest resistance (Michelmore, 2000), but subsequent studies have shown that they are also involved in shade avoidance, photomorphogenesis and development. For At5g17880, an Arabidopsis *TIR-NBS-LRR*, a role in photomorphogenic development has been shown (Faigon-Soverna *et al.* 2006).

Previously, functionally tested guanylate cyclases have been identified in Arabidopsis using a 14-amino acid long search motif deduced from an alignment of conserved and functionally assigned amino acids in the catalytic centre of annotated guanylate cyclases (Ludidi and Gehring, 2003). Recently, Gehring (2010) made use of a 14-amino acid long guanylate cyclase catalytic centre search motif modified for specificity for ATP binding and with the C-terminal metal-binding residue ([RK][YFW][DE][VIL][FV]X(8)[KR]X(1,3)[DE]) to conduct a BLAST search of the Arabidopsis genome. This motif search retrieved nine candidate Arabidopsis adenylate cyclase genes, including a gene ***(At3g04220)*** that codes for a TIR-NBS-LRR protein, as shown

in Table 1.1. Thus, it has been bioinformatically indicated that a higher plant TIR-NBS-LRR protein is also a putative adenylate cyclase.

Table 1.1: The nine bioinformatically identified *Arabidopsis thaliana* proteins containing the adenylate cyclase search motif: [RK][YFW][DE][VIL][FV]X(8)[KR]X(1,3)[DE] (Adapted from [Gehring, 2010).

ATG No.	Sequence	Annotation
At1g25240	-KWEIFEDDFCFTCKDIKE-	Epsin N-terminal homology1
At1g62590	-KFDVVISLGEKMQR--LE-	Pentatricopeptide (PPR) protein
At1g68110	-KWEIFEDDYRCFDR--KD-	Epsin N-terminal homology2
At2g34780	-KFEIVRARNEELKK-EME-	Maternal effect embryo arrest 22
At3g02930	-KFEVVEAGIEAVQR--KE-	Chloroplast protein
***At3g04220**	**-KYDVFPSFRGEDVR--KD-**	**TIR-NBS-LRR class**
At3g18035	-KFDIFQEKVKEIVKVLKD-	Linker histone-like protein-HNO4
At3g28223	-KWEIVSEISPACIKSGLD-	F-box protein
At4g39756	-KWDVVASSFMIERK--CE-	F-box protein

1.2.4 ADENYLATE CYCLASES IN HIGHER PLANTS

For many decades, the role of adenylate cyclases in synthesising cAMP from ATP has been studied in animals, microbes and plants. In contrast to the well-documented situation in the animal kingdom however, the presence of adenylate cyclases and their physiological roles in higher plant signal transduction are quite obscure (Gasumov *et al*., 1999).

Adenylate cyclases are a key component of the adenylate cyclase signalling system and catalyse the generation of cyclic adenosine monophosphate (cAMP) from ATP (Lomovatskaya, *et al*., 2008). cAMP is an ubiquitous second messenger mediating hormones and neurotransmitters, and cross-talking with other key signalling pathways of cell functions. It exerts its effects via cAMP-dependent protein kinase (protein kinase A), cAMP-gated channels, and the exchange protein directly activated by cAMP (EPAC) (Zaccolo *et al.*, 2005).

In an attempt to explain how cAMP can modulate numerous biological processes (metabolism, gene expression, cell division, cell migration, exocytosis, insulin secretion, immune response, memory formation, and cardiac contraction), suggestions have been made that parallel and spatially segregated cAMP signalling pathways coexist within the cell. According to this model, A-kinase anchoring proteins (AKAPs) anchor Protein Kinase A intracellularly in close proximity to specific modulators and targets, indicating that selective activation of individual pools of PKA requires that cAMP be made available in discrete compartments. As such, cAMP is generated by adenylate cyclases that are localised at discrete parts of the plasma membrane together with the regulatory G proteins (Zaccolo *et al.*, 2005) as is shown in Figure 1.4.

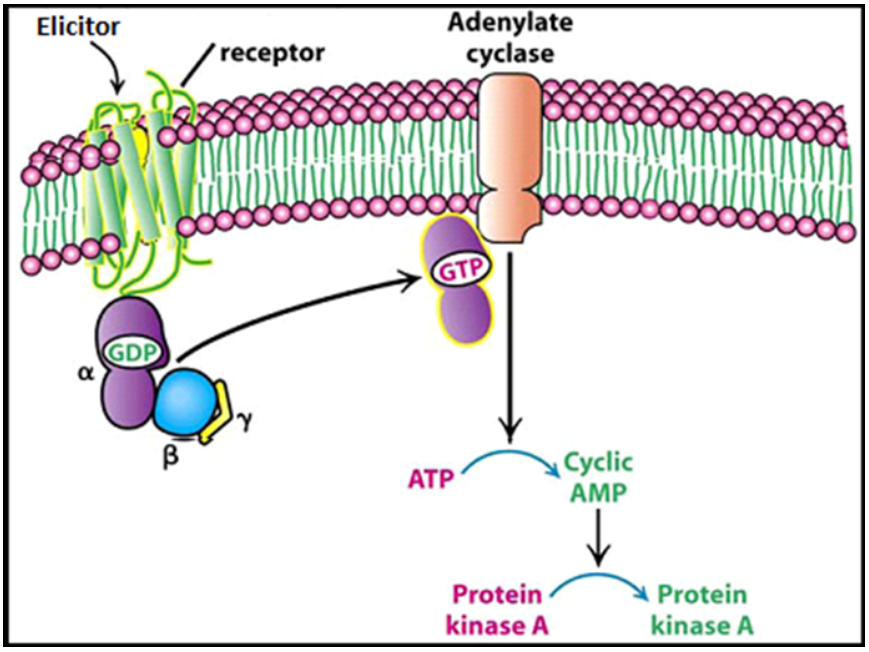

Figure 1.4: Mammalian cAMP signal transduction pathway. When the elicitor attaches to the receptor in the intracellular space, the α subunit of the G protein then attaches to the transmembrane adenylate cyclase, and thus stimulating the formation of cAMP from ATP. (Adapted from Berg *et al.*, 2007)

Although cAMP is an important signalling molecule in prokaryotes and eukaryotes, its significance in higher plants has been generally doubted because they have low adenylate cyclase activity and barely detectable amounts of cAMP (Ichikawa *et al*., 1997). There are suggestions that cAMP-phosphodiesterase activity might be relatively high, hence keeping basal cAMP levels low (Li *et al.,* 1994; Molchan *et al.,* 2000). While the role of cAMP as a secondary messenger in some plants has been proven (Ma *et al*., 2009), Hintermann and Parish (1979) came up with evidence against the occurrence of the enzyme in higher plants, and it has only slowly been accepted as part of the higher plant signalling networks (Ichikawa *et al.,* 1997). However, if the pathways of cAMP synthesis and degradation are similar in plants and animals, then one would expect to find adenylate cyclases in plants too (Assmann, 1995).

The first reported occurrence of adenylate cyclase in the tissues of higher plants was in 1970 using chromatographic analysis methods (Edman, 1975). From this finding, several similar demonstrations with a variety of plant tissues followed. However, on the grounds that the chromatographic procedures used then were not sufficiently rigorous, some critics questioned the authenticity of the identification of a radioactive product as cAMP (Chadwick and Garrod, 2009).

Others, on the basis of their own results, went further and concluded that adenylate cyclases do not occur in higher plants (Hintermann and Parish, 1979). Of the earlier studies in which positive results were obtained, only two involved the direct conversion of ATP to cAMP by a cell-free system (Al-Bader *et al*., 1976; Zeilig *et al*., 1976). More work in 1977 and 1979 succeeded in demonstrating the presence of adenylate cyclases in cell-free enzymatic preparations obtained from *Hordeum* and *Phaseolus* seedlings (Chadwick and Garrod, 2009). Still, little is known about the molecular identities of higher plant adenylate cyclases, possibly because of a high degree of sequence divergence (Talke *et al.,* 2003). In addition, the activity of adenylate cyclases in plants is very low and the enzymes are very unstable (Wilczyński, 1997).

The only annotated and experimentally confirmed adenylate cyclase in plants is a *Zea mays* pollen protein capable of generating cAMP, which in turn is a second messenger with a role in polarized pollen tube growth (Moutinho *et al.,* 2001); and this protein is structurally similar to plant TIR-NBS-LRRs (Gehring, 2010). A tissue extract method was used to quantitatively measure the level of cAMP generated from *Z. mays* pollen grain (Moutinho *et al*., 2001).

There are many predicted protein sequences homologous to the *Z. mays* pollen protein in Arabidopsis, most of which are classified as disease-resistance proteins. Those with highest

homologies correspond to two genes arranged in tandem on chromosome 3, At3g14460 and At3g14470; which is significant considering that the At3g04220 gene which encodes the putative adenylate cyclase is also located in chromosome 3. The possibility that plant adenylate cyclases might be found within a resistance gene family is interesting, especially given that cyclic nucleotides have been shown to play a role in pathogen response signalling (Talke *et al.,* 2003).

Practically, it is unlikely that a single adenylate cyclase can account for all the cAMP-dependent processes in higher plants. Given that several molecules with guanylate cyclase activity and different domains have been experimentally confirmed in *Arabidopsis thaliana*, it is likely that the same holds true for adenylate cyclases (Gehring, 2010).

Chapter 2

Materials and Methods

2.1 Isolation and Molecular Cloning of the At3g04220 Gene

2.1.1 Generation of *Arabidopsis thaliana* Plants Under Growth Conditions

Arabidopsis thaliana ecotype Columbia seeds were obtained from the Department of Biotechnology of the University of the Western Cape, South Africa. The plants were germinated in Murashige and Skoog media, then transplanted onto potting soil after 2 weeks and grown for 2 weeks thereafter under sterile growth conditions.

2.1.1.1 Surface sterilisation of *Arabidopsis thaliana* seeds

The sterilisation of the seeds was carried out under laminar flow conditions (1200 Horizontal laminar Flow Cabinet, Airvolution, Roodepoort, South Africa) using aseptic techniques. About 40 Arabidopsis seeds were transferred to a 1.5 mL microcentrifuge tube, washed with 500 µL of 70% v/v ethanol, vortexed (VX-200 Vortex Mixer, Labnet International Inc., New Jersey, USA) at medium speed for 30 seconds and the ethanol was discarded. The wash step was repeated twice. The seeds were then vortexed at medium speed in 500 µL of seed sterilisation buffer (0.1% w/v sodium dodecyl sulphate and 5% v/v chlorine bleach) for 30 seconds and the buffer was discarded. The sterilisation step was repeated twice. The seeds then underwent 5 successive washes with 1 mL of sterile distilled water (each time vortexing at medium speed for 30 seconds and discarding the water) to remove all traces of sterilisation buffer, and were finally suspended in 200 µL of sterile distilled water.

2.1.1.2 Germination and growth of *Arabidopsis thaliana* plants

Using aseptic techniques under laminar flow conditions, 10 sterile *A. thaliana* seeds were spatially distributed across a plate of Murashige and Skoog medium (0.43% w/v Murashige and Skoog powder, 3% w/v sucrose and 0.4% w/v agar at pH 5.7). Thereafter, the seeds underwent vernalisation at 4°C for 3 days before being transferred to a sterile growth chamber (Lab Companion GC -300TL Growth Chamber System, Jeio Tech, Seoul, Korea) where they were exposed to greenhouse growth conditions (average day/night temperature: 25/16°C; day/night period: 16/8 hours; 10,000 lux) for 14 days for germination and growth. The *A. thaliana* seedlings were then transplanted onto potting soil (60% v/v peat-based soil and 40% v/v vermiculite) and grown for a further 4 weeks under greenhouse growth conditions.

2.1.2 Designing and Acquisition of At3g04220-specific Primers

The genomic sequence of the At304220 gene as retrieved from TAIR (The Arabidopsis Information Resource) revealed that the At3g04220 gene contains introns, as shown by the fact that the full length genomic sequence is 3071 nucleotides long as compared to the full length copy DNA (cDNA) sequence which is 2604 nucleotides long (Figure 2.1). Hence, two sequence-specific primers (forward and reverse) were manually designed to amplify from the cDNA, with the priming sites being 50 amino acids on either side (N and C terminus) of the probable adenylate cyclase catalytic centre of the protein (Figure 2.2), in order amplify only the adenylate cyclase catalytic centre as opposed to the complete cDNA. Care was also taken to ensure that the forward primer carried the *Bam*HI restriction site and the reverse primer carried

the *Eco*RI restriction site complementary to those of the pCR®T7/NT-TOPO® expression vector (Invitrogen, Carlsbad, USA) into which the amplified gene insert was going to be cloned.

The forward primer was designed to have a 5′ GC clamp, followed by the *Bam*HI restriction site, then followed by the start codon (initiation sequence) and 15 nucleotide residues on the 5′ end of the forward priming site (Figure 2.3). The reverse primer was designed to have a 5′ GC clamp, followed by the *Eco*RI restriction site, followed by the stop codon and 15 nucleotide residues on the 3′ end. Furthermore, the primers were designed to be less than 35 base pairs long to maintain binding specificity, as shown in Figure 2.3. The manually designed primer sequences were then sent to the Molecular and Cell Biology Department of the University of Cape Town for chemical synthesis and supply.

1-50	**MDSSFLLETV AAATGFFTLL GTILFMVYRK FKDHRENKEN DSSSSTQPSP**
51-100	**SPPLSSLSLT RKYDVFPSFR GEDVRKDFLS HIQKEFQRQG ITPFVDNNIK**
101-135	**RGESIGPELI RAIRGSKIAI ILLSKNYASS SWCLD**

Figure 2.1: Amino acid sequence showing forward priming site (green), adenylate cyclase catalytic centre (red) and reverse priming site (orange)

31GCT GCT GCA ACA GGCTTC TTC ACA CTT TTG GGT ACA ATA CTT TTT ATG GTT TAC AGA AAA TTC AAA GAC CAT CGA GAA AAC AAA GAA AAT GAT TCT TCTTCT TCA ACA CAA CCG TCT CCT TCA CCA CCT CTG TCG TCT TTA TCT CTC ACG CGA **AAA TAC GAT GTC TTT CCA AGC TTC CGC GGG GAA GAT GTC CGC AAA GAC TTC CTC** AGT CAC ATT CAG AAG GAG TTT CAA AGA CAA GGA ATC ACA CCA TTT GTT GAT AAC AAT ATC AAG AGA GGA GAA TCT ATC GGT CCA GAA CTC ATT CGG GCG ATT AGA GGG TCC AAG ATC GCA ATC ATC TTG CTC TCC AAG AAC TAC GCT TCT TCA **AGC TGG TGC TTA GAC405**

Figure 2.2: Nucleotide sequence of At3g04220 gene insert showing forward priming site (in green), adenylate cyclase catalytic centre (in red) and reverse priming site (in orange).

Forward primer: **5′ *gcgcgg*AAg gat ccAATG GCT GCT GCA ACA GGC 3′**
Reverse primer: **5′ *cgcggc*gaattcTAA GTC TAA GCA CCA GCT 3′**

Figure 2.3: Nucleotide sequence of manually-designed sequence-specific primers, showing the GC clamps (italics), the *Bam* HI restriction site (small underlined letters), the start codon (red letters), the *Eco*RI restriction site (bold small underlined letters) and the stop codon (blue letters).

2.1.3 Isolation of the At3g04220 Gene from the Arabidopsis Genome via RT-PCR

The At3g04220 gene was isolated from the 6-week old *A. thaliana* plants by reverse transcriptase polymerase chain reaction (RT-PCR). Total RNA was isolated from the plants and used as the template for cDNA synthesis via reverse transcription. The cDNA thus synthesised was used as a template for isolation of the At3g04220 gene using the specific forward and reverse primers in a Polymerase Chain Reaction.

2.1.3.1 Extraction of total RNA from Arabidopsis plants

The extraction of total RNA was conducted according to the manufacturer's protocol of the QIAGEN RNeasy Plant Mini Kit (Catalogue Number 74903, Whitehead Scientific Pty Ltd, Cape Town, South Africa).

Firstly, 100 mg of fresh 6-week old *A. thaliana* leaves were flash frozen in liquid nitrogen (Afrox Industrial Gases, Ventersdorp, South Africa) and ground into powder. The plant tissue powder was decanted into an RNase-free, liquid nitrogen-cooled 2 mL microcentrifuge tube. Immediately, 450 µL of Buffer RLT was added to the tissue powder and the mixture was

vortexed vigorously to effect tissue disruption. The lysate was then incubated at 56°C for 3 minutes to further disrupt the tissue. The lysate was transferred to a QIA shredder spin column placed in a 2 mL collection tube and centrifuged for 2 minutes at 16,300 x *g*. The supernatant of the flow-through was carefully transferred to a new 2 mL microcentrifuge tube. A 0.5 volume of absolute ethanol was added to the cleared lysate and mixed immediately by pipetting. The sample was transferred to an RNeasy spin column placed in a 2 mL collection tube. The column was centrifuged for 15 seconds at 16,300 x *g* and the flow-through was discarded. Buffer RW1 (700 µL) was added to the RNeasy spin column and the column was centrifuged (Corning® LSE™ High Speed Microcentrifuge, Corning Inc., Amsterdam, Netherlands) for 15 seconds at 16,300 x *g* to wash the spin column membrane. The flow-through was discarded. Buffer RPE (500 µL) was added to the RNeasy spin column and centrifuged for 2 minutes at 16,300 x *g* to ensure that the spin column was thoroughly washed. The RNeasy column was placed in a new 2 mL collection tube and centrifuged at 16,300 x *g* for 1 minute to eliminate any possible carryover of Buffer RPE. The RNeasy spin column was placed in a new 1.5 mL collection tube. 30 µL of RNase-free water was added directly to the spin column membrane and centrifuged for 1 minute at 16,300 x *g* to elute total RNA. The total RNA was quantified using a nanodrop spectrophotometer (Nanodrop 2000, Thermo Scientific, USA) and was also resolved on a 0.8% w/v agarose gel electrophoretic system (multiSUB Mini BCMSMINI7, Biocom Ltd, Bridge of Weir, United Kingdom) for 40 minutes at 80 V to confirm its integrity.

2.1.3.2 cDNA synthesis and amplification of the *At3g04220* gene

Copy DNA was synthesised from the total RNA extracted from *A. thaliana* using reverse transcriptase and the *At3g04220* gene was amplified using *Taq* DNA polymerase via the Reverse-Transcriptase Polymerase Chain Reaction (RT-PCR) according to the manufacturer's protocol of the Thermo-Scientific Verso™ 1-Step RT-PCR Hot Start Kit (Catalogue Number AB-1455, Thermo Fisher Scientific Inc., Maryland, USA). The specifically designed forward and reverse primers were used for the amplification which was run on a thermal cycler (C1000 Touch™ Thermal Cycler, Bio-Rad Laboratories Pty Ltd, Johannesburg, South Africa).

Each 50 µl reaction contained 1 µL Verso Enzyme Mix, 25 µL 1-Step PCR Hot-Start Master Mix, 0.2 µM forward primer, 0.2 µM reverse primer, 2.5 µL Reverse Transcriptase Enhancer and 80.8 ng total RNA. The thermal cycling parameters were as follows: cDNA synthesis at 50°C for 15 minutes, Thermo-Start activation at 95°C for 15 minutes, followed by denaturation at 95°C for 20 seconds, annealing at 63.5°C for 30 seconds and extension at 72°C for 1 minute for 45 cycles, and then a final extension at 72°C for 5 minutes. The PCR product was resolved on a 1.5% w/v agarose gel at 80 V for 40 minutes against a 100 bp DNA marker (GeneRuler™ 100bp DNA Ladder, Catalogue Number SM0243, Fermentas International Inc., Maryland, USA). Visualisation of the gel was done under short wavelength UV illumination using a gel imaging system (G:BOX CHEMI EF^2, Syngene, Maryland, USA) to confirm the presence of a 408 bp DNA fragment corresponding to the partial At3g04220 gene insert.

2.1.3.3 Purification of the At3g04220 gene

The At3g04220 gene was purified from the RT-PCR mix according to the manufacturer's protocol of the Zymo Research DNA Clean and Concentrator™-5 Kit (Catalogue Number D4003, Zymo Research Corporation, California, USA). The RT-PCR product (50 µL) was mixed with 250 µL of DNA Binding Buffer in a 1.5 mL microcentrifuge tube and mixed briefly by vortexing. The mixture was transferred to a Zymo-Spin™ Column in a collection tube and centrifuged at 13,500 x *g* for 30 seconds. The flow-through was discarded. Wash Buffer (200 µL) were added to the column and centrifuged at 13,500 x *g* for 30 seconds. The wash step was repeated. Sterile warm water (30 µL) was added directly to the column matrix and incubated at room temperature for 2 minutes. The column was then transferred to a 1.5 mL microcentrifuge tube and centrifuged at 13,500 x *g* for 30 seconds to elute pure At3g04220 insert. The insert was quantified using a nanodrop spectrophotometer.

2.1.3.4 Restriction digestion of At3g04220 insert

To prepare the At3g04220 insert for ligation into the pCRT7/NT-TOPO plasmid, a double-digest restriction digestion of the insert was conducted according to the manufacturer's protocol of Fermentas *Eco*RI (Catalogue Number ER0271, Fermentas Inc., Maryland, USA)) and *Bam*HI (Catalogue Number ER0051, Fermentas Inc., Maryland, USA).

The 50 µL double-digest reaction mix was prepared as follows: 60 µl of At3g04220 insert, 40 units of *Eco* RI, 40 units of *Bam* HI and 1X Tango buffer. The digestion mix was incubated at 37°C for 4 hours then the enzymes were inactivated by heating at 80°C for 20 minutes. The digested insert was cleaned according to the manufacturer's protocol of the Zymo Research DNA Clean and Concentrator™-5 Kit (Catalogue Number D4003).

DNA Binding Buffer (500 µL) was added to the 100 µL of the double-digestion mixture in a 1.5 mL microcentrifuge tube and mixed briefly by vortexing. The mixture was transferred to a Zymo-Spin™ Column in a collection tube and centrifuged at 13,500 x *g* for 30 seconds. The flow-through was discarded. Wash Buffer (200 µL) was added to the column, centrifuged at 13,500 x *g* for 30 seconds and the flow-through was discarded. The wash step was repeated. Warm sterile water (30 µL) was added directly to the column matrix and incubated for 2 minutes. The column was then transferred to a 1.5 mL microcentrifuge tube and centrifuged at 13,500 x *g* for 30 seconds to elute pure digested *At3g04220* insert.

2.1.4 Preparation of pCR®T7/NT-TOPO®-At3g04220 Fusion Expression Construct

The commercial pCR®T7/NT-TOPO® plasmid (Invitrogen, Carlsbad, USA) was double-digested using restriction enzymes (*Bam* HI and *Eco* RI) to linearize it and also making it compatible with the double-digested *At3g04220* gene amplicon. The digested *At3g04220* gene was then ligated into the plasmid to form the pCR®T7/NT-TOPO®-At3g04220 fusion expression construct.

2.1.4.1 Restriction digestion of the pCR®T7/NT-TOPO®

A double restriction digestion of the plasmid vector was conducted according to the manufacturer's protocol using *Eco* RI (Catalogue Number ER0271, Fermentas Inc., Maryland, USA) and *Bam* HI (Catalogue Number ER0051, Fermentas Inc., Maryland, USA) in preparation for ligation.

A 100 µL double-digest reaction mix was prepared as follows: 60 µL of plasmid, 40 units of *Eco* RI, 40 units of *Bam* HI and 1X Tango buffer. The digestion mix was incubated in a water bath (WS27 SHEL LAB Shaking Water Bath, Sheldon Manufacturing Inc., Oregon, USA) at 37°C for 4 hours and then the enzymes were inactivated by heating at 80°C for 20 minutes.

The digested plasmid was purified according to the manufacturer's protocol of the Zymo Research DNA Clean and Concentrator™-5 Kit (Catalogue Number D4003) as described in Section 2.3.3.

2.1.4.2 Ligation of the At3g04220 insert into the pCRT7/NT-TOPO vector to form a pCRT7/NT-TOPO-At3g04220 expression construct

The ligation of the digested At3g04220 insert into the digested pCR®T7/NT-TOPO® plasmid was conducted according to the manufacturer's protocol of the Fermentas T4 DNA Ligase (Catalogue Number EL0011, Thermo Fisher Scientific, Maryland, USA). A final ligation reaction volume of 20 µL was made using 2 µL of the plasmid and 3 µL of the insert, 1X T4 DNA ligase buffer and 5 units of the ligase enzyme. The mixture was incubated using a dry

heating block (AccuBlock Digital Dry Bath D1100, Labnet International Inc., New Jersey. USA) at 22°C for 1 hour and then held at 4°C overnight.

The ligation product was then purified according to the manufacturer's protocol of the Zymo Research DNA Clean and Concentrator™-5 Kit (Catalogue Number D4003) as described in Section 2.3.3 to elute pure pCR®T7/NT-TOPO®-At3g04220 construct.

2.2 Expression and Purification of the Recombinant TIR-NBS-LRR Protein

2.2.1 Preparation of Competent Expression Host Cells and their Transformation with the pCR®T7/NT-TOPO®-At3g04220 Fusion Expression Construct

Escherichia coli BL21 (DE3) pLysS cells (Invitrogen™, Life Technologies, California, USA) were prepared to become chemically competent before being transformed with the pCR®T7/NT-TOPO®-At3g04220 expression construct.

2.2.1.1 Induction of chemical competence of *E. coli* BL21 (DE3) pLysS cells

A loopful of *E. coli* BL21 *(DE3)* pLysS cells from a cultured colony was inoculated into 10 mL of Luria Bertani (LB) broth supplemented with ampicillin and chloramphenicol (1% w/v

tryptone, 0.5% w/v yeast, 1% w/v sodium chloride, 0.4% w/v glucose, 100 µg/mL ampicillin and 34 µg/mL chloramphenicol) and incubated overnight at 37°C in an orbital shaker at 200 rpm to enrich the cells to the stationary phase. After the 24 hours, a fresh pre-warmed LB broth was inoculated with 1 mL of the overnight culture and incubated at 37°C in the shaker at 200 rpm while monitoring optical density at 600 nm wavelength using a visible light spectrophotometer (Spectronic™ Helios™ Epsilon™ Spectrophotometer, Thermo Electronic Scientific Instruments LLC, Wisconsin, USA). When the optical density reached 0.5 at 600 nm, signifying that the cells were in log phase, the growth of the cells was arrested by immediately incubating them on ice for 5 minutes. The culture was divided among 5 sterile 50 mL falcon tubes and the cells were collected by centrifuging at 4,000 x *g* for 5 minutes at 4°C. The supernatant was discarded the cells were re-suspended in 15 mL of ice-cold Transformation Buffer 1 (30 mM potassium acetate, 50 mM manganese chloride, 100 mM rubidium chloride, 10 mM calcium chloride, 15% v/v sterile glycerol, pH 5.8) and incubated on ice for an additional 90 minutes. The cells were harvested by centrifuging at 4,000 x *g* for 5 minutes at 4°C. After the supernatant had been discarded, the cells were re-suspended in 4 mL of ice-cold Transformation Buffer 2 (10 mM MOPS [3-(N-morpholino) propanesulfonic acid], 75 mM calcium chloride, 10 mM rubidium chloride, 15% v/v glycerol, pH 6.8). 200 µL aliquots of the competent cells were dispensed into 1.5 mL microcentrifuge tubes and flash-frozen using liquid nitrogen. The competent cells were stored at -80°C.

2.2.1.2 Transformation of chemically competent *E. coli* BL21 (DE3) pLysS cells

10 µL of the pCR®T7/NT-TOPO®-At3g04220 construct was transferred to a cold and sterile 1.5 mL microcentrifuge tube and incubated on ice while the competent cells were thawed on ice and

gently resuspended. 100 µL of the cell suspension were carefully transferred to the construct solution and gently mixed before being incubated on ice for 20 minutes. Thereafter, the mixture was heat shocked through incubation at 42°C for 90 seconds in a water bath before being incubated on ice for 5 minutes. The transformation mixture was supplemented with 500 µL of Super Optimal Broth With Catabolite Repression (SOC) medium (2% w/v tryptone, 0.5% w/v yeast extract, 10 mM sodium chloride, 2.5 mM potassium chloride, 10 mM magnesium chloride, 10 mM magnesium sulphate, 20 mM glucose) and incubated for 90 minutes at 37°C in an orbital shaker at 200 rpm to increase transformation efficiency. Using the spread plate method, 100 µL aliquots of the transformation mixture were inoculated onto LB broth supplemented with ampicillin and chloramphenicol (1% w/v tryptone, 0.5% w/v yeast, 1% w/v sodium chloride, 100 µg/mL ampicillin [Catalogue Number BIO-87025, Bioline, London, United Kingdom], 34 µg/mL chloramphenicol [Catalogue Number BIO-87027, Bioline, London, United Kingdom]). A negative control was also included by substituting the recombinant vector with non-recombinant vector. The plates were incubated at 37°C overnight and then analysed for growth of transformant cell colonies.

2.2.2 Determination of the Cloning and Transformation Success

The success of the cloning and transformation processes was determined by pilot recombinant protein expression. The transformants were enriched in double-strength yeast tryptone medium and TIR-NBS-LRR adenylate cyclase expression was induced using IPTG. Stable transformants were then determined using sodium dodecyl sulphate polyacrylamide gel electrophoresis (SDS-

PAGE), and the positive recombinants thus determined were further verified via colony PCR and restriction double digest analysis.

2.2.2.1 Enrichment and induction of transformants

Transformants (200 µL) were inoculated into 10 mL of double-strength yeast-tryptone (2YT) medium supplemented with ampicillin and chloramphenicol (1.6% w/v tryptone, 1% w/v yeast extract, 0.5% w/v sodium chloride, 0.4% w/v glucose, 100 µg/mL ampicillin, 34 µg/mL chloramphenicol; pH 7.0) and incubated overnight at 37°C in an orbital shaker at 200 rpm. Thereafter, 400 µL of the enriched overnight culture was inoculated into 10 mL of fresh 2YT medium supplemented with ampicillin and chloramphenicol and incubated at 37° C in an orbital shaker at 200 rpm until the optical density at 600 nm had reached 0.5 (using 2YT medium as the blank). Expression of the recombinant TIR-NBS-LRR adenylate cyclase protein was then induced using 1 mM isopropyl-β-D-1-thiogalactopyranoside (IPTG, Catalogue Number BIO-37036, Bioline, London, United Kingdom) and further incubation under the same conditions for 3 additional hours. Aliquots of cells from zero and each subsequent hour were harvested by centrifugation at 6,500 x *g* for 5 minutes and discarding the supernatant.

2.2.2.2 Determination of positive clones via SDS-PAGE

The induced transformants were re-suspended in 500 µL of sterile distilled water using a vortex mixer at high speed for 3 minutes. A 40 µL aliquot of the cells was suspended in 1X protein loading buffer (20% v/v glycerol, 0.1 M Tris hydrochloride, 2% w/v sodium dodecyl sulphate, 0.1% w/v Bromophenol Blue and 20% v/v β-mercaptoethanol) and 20 mL aliquots of the

samples were loaded onto the polyacrylamide gel after boiling at 95°C for 5 minutes. The samples were concentrated on a 5% Stacking Gel (4.8% v/v acrylamide, 0.1% w/v sodium dodecyl sulphate, 0.125 M Tris-hydrochloride, 0.05% w/v ammonium persulphate, 0.4% v/v TEMED) before being resolved on a 12% running gel (12% v/v acrylamide stock, 0.1% w/v SDS, 0.375 M Tris-hydrochloride, 0.05% w/v ammonium persulphate, 0.2% v/v TEMED) at 120 V for 1 hour using an ENDURO™ Modular Vertical Gel System (Labnet International Inc., New Jersey, USA) against a 100 kDa protein marker (PageRuler Unstained Low Range Protein Ladder, Catalog Number 26632, Thermo Fisher Scientific Inc., Illinois, USA) in 1X Protein Running Buffer (1.44% w/v glycine, 0.3% w/v Tris-hydrochloride, 0.1% w/v sodium dodecyl sulphate) for 2 hours. The gel was then stained using the staining buffer (10% v/v ethanol, 10% v/v methanol, 10% v/v acetic acid, 0.5% w/v Coomassie powder) for 15 minutes on a rocker (UltraRocker™ Rocking Platform, Bio-Rad, Johannesburg, South Africa) at 100 rpm at room temperature. Thereafter, the staining solution was drained off and the gel de-stained using the de-staining buffer (10% v/v ethanol, 10% v/v methanol, 10% v/v acetic acid) under the same conditions. The gel was visually analysed for a band of 17.64 kDa corresponding to the recombinant TIR-NBS-LRR adenylate cyclase protein.

2.2.2.3 Verification of recombinants via alkaline lysis and double digestion

An overnight culture of the transformants that had shown an expression of the recombinant TIR-NBS-LRR protein was enriched according to the method described in Section 2.2.2.1 in preparation for the isolation of the pCR®T7/NT-TOPO®-At3g04220 expression construct. The cells were then collected by centrifuging at 12,750 x *g* for 5 minutes and the supernatant discarded. The pellet thus collected was re-suspended in 400 µL of ice-cold GTE (50 mM

glucose, 25 mM Tris-hydrochloride, pH 8.0, 100 mM ethylenediaminetetraacetic acid [EDTA]). This mixture (200 µL) was mixed with 400 µL ice-cold NaOH/SDS (0.2 M sodium hydroxide, 1% w/v sodium dodecyl sulphate) by inversion in 2 mL microcentrifuge tubes and incubated on ice for 5 minutes. The mixture was centrifuged at 9,200 x *g* for 5 minutes and the supernatant was transferred to new 2 mL microcentrifuge tubes. 10% of the final volume of supernatant and 60% of the final volume of supernatant of potassium acetate solution (1 M potassium acetate and 1.9 M acetic acid) and absolute ethanol respectively were added to the supernatant. The mixture was incubated overnight at -20°C to allow precipitation of the construct. Thereafter, the mixture was centrifuged at 9,200 x *g* for 5 minutes to collect the pellet and the supernatant was discarded. The pellet was washed with 500 µL of ice-cold 70% v/v ethanol and gently re-suspended in the ethanol by pipetting. The mixture was centrifuged at 9,200 x *g* for 2 minutes; and the wash step was repeated. After centrifugation, the supernatant was discarded and the pellet dried at room temperature to remove the excess ethanol.

A total of 2 µL of the construct suspension was then digested with 20 units of *Eco*R1, 20 units of *Bam*H1, and 2X Tango buffer in a 50 µL reaction at 37°C for 4 hours. The enzymes were inactivated by heating at 80°C for 20 minutes and then the digested construct and insert were cleaned according to the manufacturer's protocol of the Zymogen DNA Clean and Concentrator™-5 Kit (Catalogue Number D4003). The construct and insert were resolved on a 0.8% w/v agarose gel against both a 1 kb and a 100 bp DNA marker to visualise the bands corresponding to the expected 2870 bp digested plasmid and the 404 bp excised insert.

2.2.2.4 Verification of recombinants via confirmatory colony PCR

A 10 mL overnight culture from each transformant colony that had shown an expression of the recombinant TIR-NBS-LRR protein was made by inoculating 2YT media supplemented with 100 µg/mL ampicillin and 34 µg/mL chloramphenicol with a few cells from each colony. The pCR®T7/NT-TOPO®-At3g04220 expression construct was isolated from the transformants according to the alkaline lysis method described in Section 3.2.3. The isolated construct was then used as template for colony PCR and according to the manufacturer's protocol of the Thermo-Scientific Verso™ 1-Step RT-PCR Hot-Start Kit. The PCR mix was made as follows: each 50 µL reaction contained 1 µL Verso Enzyme Mix, 25 µL 1-Step PCR Hot-Start Master Mix, 0.2 mM forward primer, 0.2 mM reverse primer, 2.5 µL Reverse Transcriptase Enhancer and 1 µL pCR®T7/NT-TOPO®-At3g04220. The thermal cycling parameters were as follows: activation at 95°C for 15 minutes, followed by denaturation at 95°C for 20 seconds, annealing at 63.5°C for 30 seconds and extension at 72°C for 1 minute for 45 cycles, followed by a final extension at 72°C for 5 minutes. The PCR product was resolved on a 1.5% w/v agarose gel at 80V for 40 minutes against a 100 bp DNA marker. Visualisation of the gel was done under short wavelength UV illumination using a gel imaging system to confirm the presence of a 408 bp DNA fragment corresponding to the At3g04220 gene insert.

2.2.3 Determination of Solubility of the Recombinant TIR-NBS-LRR Protein Under Native Conditions

The solubility of the recombinant TIR-NBS-LRR protein under native conditions was determined by lysing the recombinant cells and analysing the protein components of the lysate by SDS-PAGE.

2.2.3.1 Cell lysis using lysozyme

LB broth (10 mL) supplemented with 100 µg/mL ampicillin and 34 µg/mL chloramphenicol were inoculated with a loopful of the recombinant cells and incubated at 37°C overnight in an orbital shaker at 200 rpm. Thereafter, 400 µL of the enriched overnight culture was inoculated into 10 mL of fresh LB broth supplemented with ampicillin and chloramphenicol and incubated at 37° C in an orbital shaker at 200 rpm until the optical density at 600 nm had reached 0.5 (using LB broth medium as the blank). Expression of the recombinant TIR-NBS-LRR adenylate cyclase protein was then conducted by expression induction using 1 mM IPTG and further incubation under the same conditions for 3 additional hours. The induced culture (1 mL) was centrifuged at 9,200 x *g* for 5 minutes. The supernatant was discarded and the cells were re-suspended in 500 µL of sterile Tris-buffered saline (TBS) Solution supplemented with phenylmethylsulfonyl fluoride (PMSF) solution (50 mM Tris, 150 mM sodium chloride, 1 mM PMSF pH 7.5) and 0.5 mg/µL lysozyme (Fluka Catalogue Number 62970, Sigma-Aldrich Pty Ltd, Johannesburg, South Africa). The cell lysis mixture was incubated on ice for 1 hour and then vortexed at high speed for 10 minutes with 1 minute intervals of incubation on ice. The lysis mixture was then centrifuged at 9,200 x *g* for 2 minutes and a 40 µL aliquot of the supernatant (soluble protein fraction) was analysed for the presence of the TIR-NBS-LRR

protein via SDS-PAGE and according to the method described in Section 3.2.2. The presence of the protein in the lysate indicates that the protein is soluble and is in its native condition.

2.2.4 Purification of TIR-NBS-LRR Protein Under Native Non-Denaturing Conditions

The TIR-NBS-LRR protein was purified from the *E. coli* BL21 (DE3) pLysS expression host according to the manufacturer's protocol of the HIS-Select® Nickel Affinity Gel (Catalogue Number P6611, Sigma-Aldrich, Missouri, USA) under native non-denaturing conditions.

2.2.4.1 Equilibriation of the nickel affinity gel

A 100 µL aliquot of HIS-Select® Nickel Affinity Gel beads was allowed to settle at room temperature before 50 µL of 30% ethanol was removed. The beads were equilibriated using 500 µL of Equilibriation Buffer (0.1 M sodium phosphate, 8 M urea, pH 8.0). The equilibriation mixture was shaken on an orbital shaker (Stuart Mini Orbital Shaker SSM1, Bibby Scientific Limited, Staffordshire, United Kingdom) at 170 rpm for 3 minutes, then further equilibriated on a rotary mixer (Revolver, Labnet International Inc., New Jersey, USA) for 15 minutes at room temperature. The beads were allowed to settle for 5 minutes at room temperature and the Equilibriation Buffer was removed.

2.2.4.2 Binding of TIR-NBS-LRR protein to Nickel Affinity Gel

The 25 mL of lysate from Section 3.3.1 was mixed with 5 mL of the beads and the protein was allowed to bind to the Nickel Affinity Gel for an hour at room temperature on a rotary mixer. The binding mixture was then centrifuged at 2,300 x *g* for 30 seconds. The beads were allowed to settle for 5 minutes and the supernatant removed. The beads were washed twice with Wash Buffer (0.1 M sodium phosphate, 8 M urea, pH 6.3) to remove unbound protein.

2.2.4.3 Elution of TIR-NBS-LRR from Nickel Affinity Gel

Beads (500 µL) were transferred to a new 1.5 mL microcentrifuge tube, allowed to settle and all residual Wash Buffer was removed. The beads were re-suspended in 1 mL of Elution Buffer (8 M urea, 100 mM NaH_2PO_4, 10 mM Tris hydrochloride: pH 8.0, 500 mM sodium chloride, 20 mM β-mercaptoethanol, 15% v/v glycerol, 250 mM Imidazole, 0.5 mM PMSF, pH 7.4) and incubated for 20 minutes at room temperature. The elution mixture was then mixed on a rotary mixer for 15 minutes at 4°C. The tubes were spun on a minifuge (LabnetSpectrafuge Mini Centrifuge Model C1301B, Labnet International, New Jersey, USA) for a few seconds to settle the beads. The eluent (pure TIR-NBS-LRR) was transferred into a new 1.5 mL microcentrifugetube and quantified using a nanodrop spectrophotometer before being stored at -20°C.

2.3 Activity Assaying and Functional Characterization of the Recombinant TIR-NBS-LRR Protein

2.3.1 Endogenous Assaying of the Adenylate Cyclase Activity of the Recombinant TIR-NBS-LRR Protein

An endogenous assay to determine the adenylate cyclase activity of the TIR-NBS-LRR catalytic centre was conducted by inducing TIR-NBS-LRR expression with 1 mM IPTG and supplementing the culture with either sterile distilled water, forskolin or dideoxyadenosine followed by an assessment of the levels of cAMP generated after a two-hour growth period by enzyme immunoassay (cAMP Enzyme Immunoassay Kit, Catalogue Number CA201, Sigma, Missouri, USA). The endogenous assay was conducted in triplicate and the results were subjected to Analysis of Variance (Super-Anova, Stats Graphics Version 7, 1993, Stats graphics Corporation, USA).

2.3.1.1 TIR-NBS-LRR induction, activation and inhibition

A 10 mL overnight culture of recombinant cells was made according to the protocol described in Section 3.2.1. The overnight culture (2 mL) was inoculated into 100 mL of fresh double-strength yeast-tryptone media and incubated at 37°C at 200 rpm up until the optical density at 600 nm had reached 0.5. The culture was then split into four equal portions of 20 mL aliquots and treated as shown in Table 4.1 below, and then allowed to incubate at 37°C for 2 hours at 200 rpm. IPTG was added to induce protein expression, 3-isobutyl-1-methyl xanthine (IBMX) was added to

inhibit cAMP degradation by phosphodiesterases, forskolin was added to activate adenylate cyclase activity and dideoxyadenosine was added to inactivate adenylate cyclase activity. The cells were harvested by centrifugation at 16,300 x *g* for 5 minutes and the pellets stored at -20°C.

Table 2.1: Induction, activation and inhibition of the recombinant TIR-NBS-LRR adenylate cyclase protein

	Tube 1	**Tube 2**	**Tube 3**	**Tube 4**
IPTG	-	1 mM	1 mM	1 mM
IBMX	1 mM	1 mM	1 mM	1 mM
Forskolin	-	-	100 µM	-
Dideoxy-adenosine	-	-	-	100 µM

2.3.1.2 Recombinant cell lysis and enzyme immunoassay

Lysis Buffer 1 (1 mL) (Amersham Healthcare, USA) supplemented with 2 mM IBMX was added to the cell pellets from Section 4.1.1. The cells were lysed on an orbital shaker at 200 rpm at room temperature for 1 hour. The lysate was centrifuged at 16,300 x g for 5 minutes to spin down any precipitate. A 200 µL aliquot of the supernatant was mixed with 200 µL of Lysis Buffer 2 (Amersham Healthcare, USA). The cAMP in this mixture was then acetylated by adding the acetylating reagent (triethylamine: acetic anhydride 2:1 v/v) at a volumetric ratio of 1:20 acetylating reagent:sample. The mixture was vortexed at high level for 2 seconds respectively and the cAMP level measured by enzyme immunoassay in accordance with the manufacturer's protocol.

2.3.2 *In vitro* Assay of Adenylate Cyclase Activity of TIR-NBS-LRR

An *in vitro* assay to determine the adenylate cyclase activity of the purified TIR-NBS-LRR adenylate cyclase protein was conducted via enzyme immunoassay and according to the manufacturer's protocol of the cAMP Enzyme Immunoassay Kit (Catalogue Number CA201, Sigma, Missouri, USA). The assay included characterization of the effect of different ions and molecules (GTP, Mg^{2+}, Mn^{2+}, Ca^{2+}, CO_3^{2-}) on the biological activity of the purified protein. The *in vitro* assay was conducted in triplicate and the results subjected to Analysis of Variance (Super-Anova, Stats Graphics Version 7, 1993, Stats Graphics Corporation, USA).

2.3.2.1 Preparation of samples and enzyme immunoassay

Several 200 µL reaction mixes for the *in vitro* assay were made in 1.5 mL microcentrifuge tubes with the purified protein from Section 3.4.3 and as is shown in Table 2.2 below. Each tube contained 50 mM Tris HCl pH 8.0 for buffering action, 2 mM IBMX to prevent phosphodiesterase degradation of cAMP and 25 µg of purified TIR-NBS-LRR (except in the control). Each reaction mix was incubated at room temperature for 20 minutes and the reaction was stopped by adding 1 mM EDTA to chelate all the metal ions and hence remove the co-factors necessary for the reaction. The samples were also boiled for 5 minutes in order to inactivate the protein. The samples were then clarified by centrifugation at 16,300 x *g* for 5 minutes. The cAMP was then acetylated by adding the acetylating reagent (triethylamine: acetic anhydride 2:1 v/v) at a volumetric ratio of 1:20 acetylating reagent:sample. The mixture was vortexed at high level for 2 seconds respectively and the cAMP level then measured by enzyme immunoassay and in accordance with the manufacturer's protocol.

Table 2.2: Molecular characterization of the recombinant TIR-NBS-LRR

	Tube 1	**Tube 2**	**Tube 3**	**Tube 4**	**Tube 5**	**Tube 6**	**Tube 7**	**Tube 8**
Tris	50 mM	50 mM	50 mM	50 mM	50 mM	50 mM	50 mM	50 mM
IBMX	2 mM	2 mM	2 mM	2 mM	2 mM	2 mM	2 mM	2 mM
$MgCl_2$	5 mM	5 mM	-	5 mM	5 mM	5 mM	5 mM	5 mM
Protein	-	25 µg	25 µg	25 µg	25 µg	25 µg	25 µg	25 µg
ATP	1 mM	1 mM	1 mM	1 mM	1 mM	1 mM	-	1 mM
$MnCl_2$	-	-	5 mM	-	-	-	-	-
$CaCl_2$	-	-	-	100 µM	-	-	-	-
GTP	-	-	-	-	-	5 mM	5 mM	-
$NaHCO_3$	-	-	-	-	50 mM	-	-	-

2.3.3 *In vivo* Assay of the Adenylate Cyclase Activity of TIR-NBS-LRR

The ability of the recombinant TIR-NBS-LRR to produce cAMP from ATP *in vivo* was determined via a complementation test of the mutant *E. coli cya*A SP850 host strain (Coli Genetic Stock Center, Yale University, Connecticut, USA) with the pCR®T7/NT-TOPO®-At3g04220 expression host, followed by screening for a selectable marker.

2.3.3.1 Preparation of competent *E. coli cya*A SP850 mutant cells

Competent *E. coli cya*A SP850 cells were prepared according to the protocol described in Section 3.1.1, replacing ampicillin and chloramphenicol with 15 µg/mL kanamycin.

2.3.3.2 Transformation of competent *E. coli cya*A SP850 mutant cells with pCR®T7/NT-TOPO®-At3g04220 expression construct and the pCR®T7/NT-TOPO® empty vector

Competent *E. coli cya*A SP850 cells were transformed with the pCR®T7/NT-TOPO®-At3g04220 construct and the pCR®T7/NT-TOPO® empty vector according to the protocol described in Section 3.1.2, replacing chloramphenicol with 15 µg/mL kanamycin.

2.3.3.3 Determination of adenylate cyclase activity

A MacConkey agar plate supplemented with 15 µg/mL kanamycin and 0.1 mM IPTG was divided in to four sectors, as is shown in Figure 2.4 below. Using the streak-plate method, mutant *E. coli cya*A SP850 cells, recombinant *E. coli cya*A SP850 cells carrying the recombinant pCR®T7/NT-TOPO®-At3g04220 plasmid, as well *E. coli cya*A SP850 cells carrying the empty

pCR®T7/NT-TOPO® plasmid were each inoculated onto the respective plate sectors. After a 36-hour incubation at 37°C, the plates were visually analysed for phenotypic characteristics.

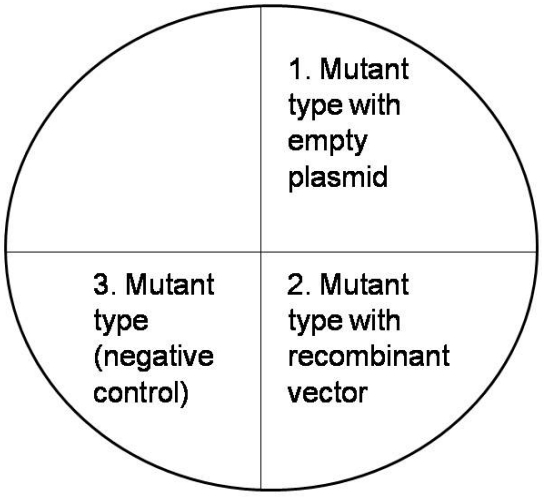

Figure 2.4: Distribution of *cyaA* mutant cells on MacConkey agar plates. (1) Sector 1 contains *cya*A mutants carrying the empty plasmid. (2) Sector 2 contains *cya*A mutants carrying the *At3g04220* gene fragment. (3) Sector 3 contains the *cya*A mutant cells.

Chapter 3

Results, Discussion and Conclusions

3.1 RESULTS

3.1.1 Bioinformatic Analysis of the At3g04220 Gene

The At3g04220 gene is expressed at low level during the 13 growth stages of *A. thaliana* and has been isolated from the hypocotyl once (NCBI, 2012). The At3g04220 gene is located on chromosome 3 of the *Arabidopsis* genome between positions 1,109,118 and 1,112,188 on the reverse strand and is 3071 base pairs in length. However, the gene contains 5 exons and 4 introns as shown in Figure 3.2 and its copy DNA (cDNA) sequence is 2604 base pairs long. It is flanked by genes At3g04181, At3g04184, At3g04190 (manganese binding), At3g04200, At3g04210 (TIR-NBS-LRR transmembrane receptor activity), At3g04230 (structural constituent of ribosome) and At3g04240 [Ensembl Genome Browser, 2012] as is shown in Figure 3.1.

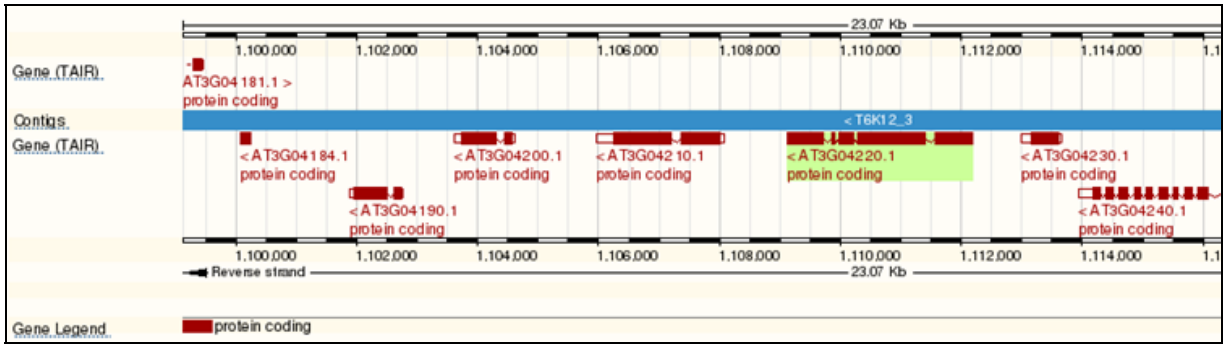

Figure 3.1: Locus of At3g04220 (highlighted in green) in *Arabidopsis* genome in relation to its flanking genes (Adapted from Ensembl Genome Browser, 2012).

At3g04220 is co-expressed with At3g17690 (cyclic nucleotide-gated channel), At3g23250 (defense response and growth factor signal transduction), At3g28580 (ATP binding), At1g80820

(defense and cold response), At5g22540 (hyperosmotic salinity response), At5g22530 (systemic acquired resistance), At5g03800 (embryo development), At5g38340 (TIR-NBS-LRR transmembrane receptor) and At5g38350 (TIR-NBS-LRR protein) (Biological Linked Open Database, 2012).

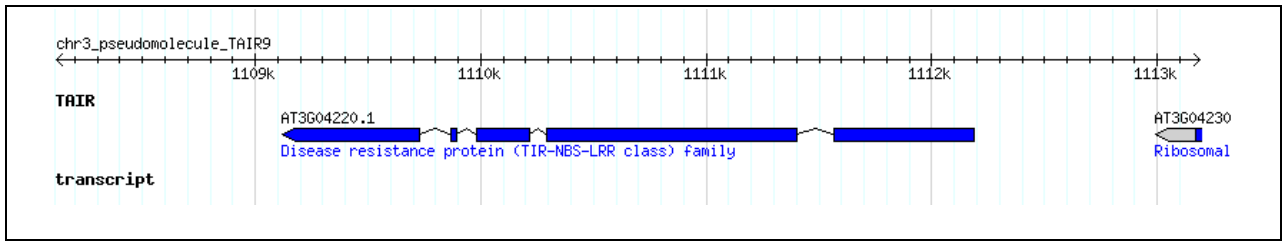

Figure 3.2: Gene splicing structure of At3g04220 (Adapted from MIPS, 2012).

The At3g04220 gene's only transcript is a disease resistance protein from the TIR-NBS-LRR family in the Arabidopsis genome that is made up of 867 amino acids (Qutob *et al.*, 2006; TAIR, 2012) as shown in Figure 3.3; and the probable adenylate cyclase catalytic centre is located from amino acid number 61 to number 77. The ATP binding and hydrolysis centres of the TIR-NBS-LRR protein are found between amino acids 257 and 398 within the NBS domain.

1 MDSSFLLETV AAATGFFTLL GTILFMVYRK FKDHRENKEN DSSSSTQPSP
51 SPPLSSLSLT R**KYDVFPSFR GEDVRKD**FLS HIQKEFQRQG ITPFVDNNIK
101 RGESIGPELI RAIRGSKIAI ILLSKNYASS SWCLDELVEI IKCKEEMGQT
151 VIVIFYKVDP SLVKKLTGDF GKVFRNTCKG KERENIERWR EAFKKVATIA
201 GYDSRKWDNE SGMIEKIVSD ISEMLNHSTP SRDFDDLIGM GDHMEKMKPL
251 LDIDSD***EMKT IGIWGPPGVG KTTIARSLYN QHSDKFQLSV FMESIKTAYT***
301 IPACSDDYYE KLQLQQRFLS QITNQENVQI PHLGVAQERL NDKKVLVVID
351 DVNQSVQVDA LAKENDWLGP GSRIIITTQD RGILRAHGIE HIYEVDYPNY
401 EEALQIFCMH AFGQKSPYDG FEELAQQVTT LSGRLPLGLK VMGSYFRGMT
451 KQEWTMALPR VRTHLDGKIE SILKLSYDAL CDVDKSLFLH LACSFHNDDT
501 ELVEQQLGKK FSDLRQGLHV LAEKSLIHMD LRLIRMHVLL AQLGREIVRK
551 QSIHEPGQRQ FLVDATDIRE VLTDDTGSRS VIGIDFDFNT MEKELDISEK
601 AFRGMSNLQF IRIYGDLFSR HGVYYFGGRG HRVSLDYDSK LHFPRGLDYL
651 PGKLSKLEKL WEGIQPLRNL EWLDLTCSRN LKELPDLSTA TNLQRLSIER
701 CSSLVKLPSS IGEATNLKKI NLRECLSLVE LPSSFGNLTN LQELDLRECS
751 SLVELPTSFG NLANVESLEF YECSSLVKLP STFGNLTNLR VLGLRECSSM
801 VELPSSFGNL TNLQVLNLRK CSTLVELPSS FVNLTNLENL DLRDCSSLLP
851 SSFGNVTYLK RLKFYKC

Figure 3.3: Amino acid sequence for TIR-NBS-LRR encoded by At3g04220 highlighting the probable adenylate cyclase catalytic centre (underlined) and the ATP binding and hydrolysis centre (italicised) (Adapted from TAIR, 2012)

This gene encodes an annotated transmembrane receptor, nucleoside-triphosphatase activity, and nucleotide binding. It is involved in signal transduction, defence response, apoptosis and innate immune response; and is localised intrinsic to the plasma membrane (TAIR, 2012).

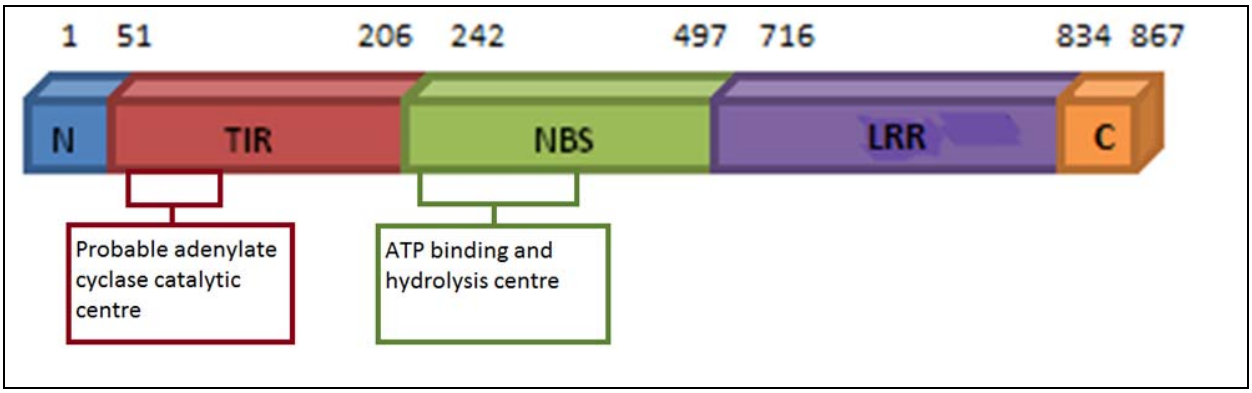

Figure 3.4: Domain organisation of TIR-NBS-LRR protein encoded by the At3g04220 gene showing probable adenylate cyclase catalytic centre; and ATP binding and hydrolysis centre (Adapted from TAIR, 2012). **NB**. Not to scale

According to the Psi-pred Protein Structure Prediction Server (2012) of the University College London, the TIR-NBS-LRR protein encoded by At3g04220 has an extracellular domain of the first 13 amino acids from the N-terminal, a transmembrane domain of amino acid positions 16 to 31, and a cytoplasmic domain from amino acid number 32 onwards to the carboxy terminal.

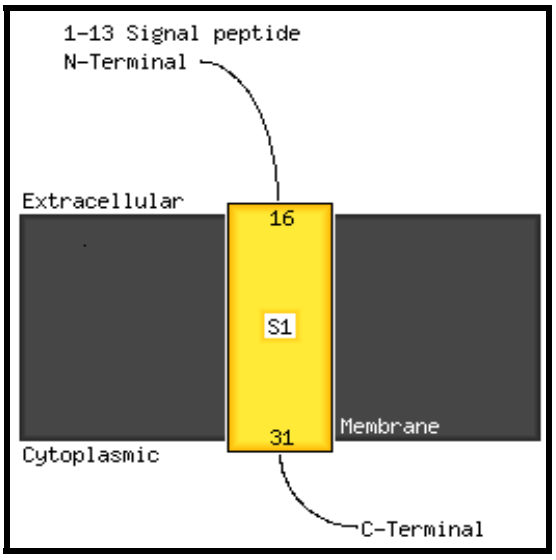

Figure 3.5: Transmembrane topology of TIR-NBS-LRR protein encoded by the *At3g04220* gene (Psi-pred, 2012)

The Phyre^2 Protein Fold Recognition Server predicts that the TIR-NBS-LRR protein encoded by At3g04220 is similar in structure to the protein encoded by the At1g72930 gene from *A. thaliana* at a 100 percent confidence level. The three-dimensional structure of TIR-NBS-LRR as predicted by Phyre^2 is shown in Figure 1.10 to have predominantly eight alpha helical regions, three beta sheet regions and thirteen randomly coiled regions.

Alignment coverage by the Phyre^2 Protein Fold Recognition Server (Kelley and Sternberg, 2009) software predicts, at higher than the 99.7 percent confidence level, that certain sequences within

the TIR-NBS-LRR protein are aligned to those in proteins with known function in apoptosis, ATP binding, ATPase activity, signalling, replication, protein binding, immunity and the cell cycle, as is shown in Table 1.2 (Kelley and Sternberg, 2009).

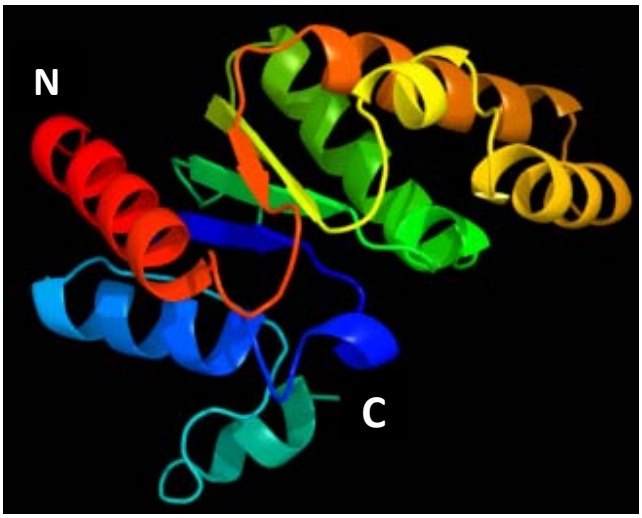

Figure 3.6: Predicted three-dimensional model of TIR-NBS-LRR coloured by rainbow N-C terminus (Kelley and Sternberg, 2009)

Apart from being intrinsic to the cell membrane, the His-tagged recombinant TIR-NBS-LRR fusion protein is predicted to have a 91.3 percent chance of solubility when overexpressed in *E. coli* (Harrison, 2000) because it contains 11 Arginine (R), 5 Asparagine (N), 12 Aspartic Acid (D), 6 Glutamic Acid (E), 12 Glycine (G), 10 Lysine (K), 7 Proline (P) and 19 Serine (S) residues (Recombinant Protein Solubility Prediction, 2012). The expressed fusion protein is a truncated form of the gene product of At3g04220 and includes the polyhistidine region and the Xpress™ epitope from the expression vector, pCR®/T7-NT-TOPO®, and the adenylate cyclase catalytic centre as shown in Figure 1.11.

MRGSHHHHHHGMASMTGGQQMGRDLYDDDDKAAATGFFTLLGTILFMVYRKFKDHRENKENDSSSSTQPSPSPPL
SSLSLTRKYDVFPSFRGEDVRKDFLSHIQKEFQRQGITPFVDNNIKRGESIGPELIRAIRGSKIAIILLSKNYASSSWCLD

Figure 3.7: Primary structure of recombinant TIR-NBS-LRR segment where **M** is the methionine encoded by the start codon (ATG), **H**is polyhistidine region (6xHis tag) and **D** is the Xpress™ epitope and the adenylate cyclase catalytic centre is underlined

At3g04220 is one of the $NLPp_p$ (necrosis and ethylene-inducing peptide1-like proteins from *Phytophora sojae*) or flg22-induced genes with known or putative roles in immunity-related signal perception, signal transduction, and pathogen defence execution (Qutob *et al*., 2006). It has been shown to be exclusively up-regulated by salt stress in plant roots as well (Ma, Gong and Bohnert, 2006).

At3g04220 is one of the bioinformatically proposed higher plant adenylate cyclases which has not been characterised as yet, and hence its isolation and characterisation using molecular biology techniques will provide insights into the physiological roles of TIR-NBS-LRR in plant disease resistance and tolerance.

Table 3.1: Alignment coverage of proteins containing sequences similar to those of TIR-NBS-LRR at 99.7+ confidence level (Adapted from Kelley and Steinberg, 2009)

Template	Gene/Protein	Alignment residues	Alignment coverage	Template information	Function
c3jrnA	At1g72930	62-226		Crystal structure of TIR domain from *A. thaliana*	Plant protein
c3oziB	L6tr	62-226		Crystal structure of TIR domain from flax disease resistance2 protein l6	Plant protein
c2a5yB	Ced-4	164-552		Structure of ced-4/ced-9 complex	Apoptosis
c1z6tC	Apoptotic protease-activating factor 1	164-551		Structure of apoptotic protease-activating factor 12 bound to ADP	Apoptosis
c1fnnB	Cell division control protein 6	229-551		Crystal structure of cdc6p from *Pyrobaculum aerophilum*	Cell cycle
c2fnaA	Conserved hypothetical protein	225-544		Crystal structure of an archael AAA+ ATPase from *Sulfolobus solfataricus* p2	ATP-binding protein
c3h16A	TIR protein	60-171		Crystal structure of a bacterial TIR domain, pdTIR from *Paracoccus denitrificans*	Signaling protein
c2qbyB	Cell division control protein 6 homolog 3	230-542		Crystal structure of a heterodimer of cdc6/orc1 initiators from *S. solfataricus*	Replication

3.1.2 Isolation of the At3g04220 Gene and the Expression and Purification of its Recombinant Product

The partial At3g04220 gene containing the adenylate cyclase domain was amplified from *A. thaliana* total RNA by reverse transcriptase polymerase chain reaction (RT-PCR) using At3g04220 sequence-specific primers (Figure 5.1A). The gene fragement and the pCR®T7/NT-TOPO® vector were double-digested using the *Bam*HI and *Eco*RI restriction endonucleases in preparation for ligation of the gene insert into the vector. The amplified gene fragment was cloned into the pCR®T7/NT-TOPO® expression vector. The pCR®T7/NT-TOPO® expression vector was chosen over other expression vectors because it encodes a 6xHis tag which is essential for the protein purification process in which a nickel affinity gel was then used to isolate the recombinant TIR-NBS-LRR protein from the total protein of the expression host. The His tag was desirable over other affinity tags because it adds a very short fragment to the recombinant fusion protein, thus minimising the possibility of interference with soluble expression and native purification (Figure 3.7). Following cloning, the pCR®T7/NT-TOPO®-partial-At3g04220 construct was transformed into competent *E. coli* BL21 (DE3) pLysS cells and the partial gene expressed as the recombinant TIR-NBS-LRR adenylate cyclase protein. In order to confirm if the correct insert was cloned, a confirmatory colony PCR was undertaken using the same set of sequence specific primers to re-amplify the At3g04220 gene fragment (Figure 3.8B). The recombinant TIR-NBS-LRR adenylate cyclase protein was fully expressed in *E. coli* BL21 (DE3) pLysS (Figure 3.8C) and then purified using an Ni-NTA affinity matrix (Figure 3.8D).

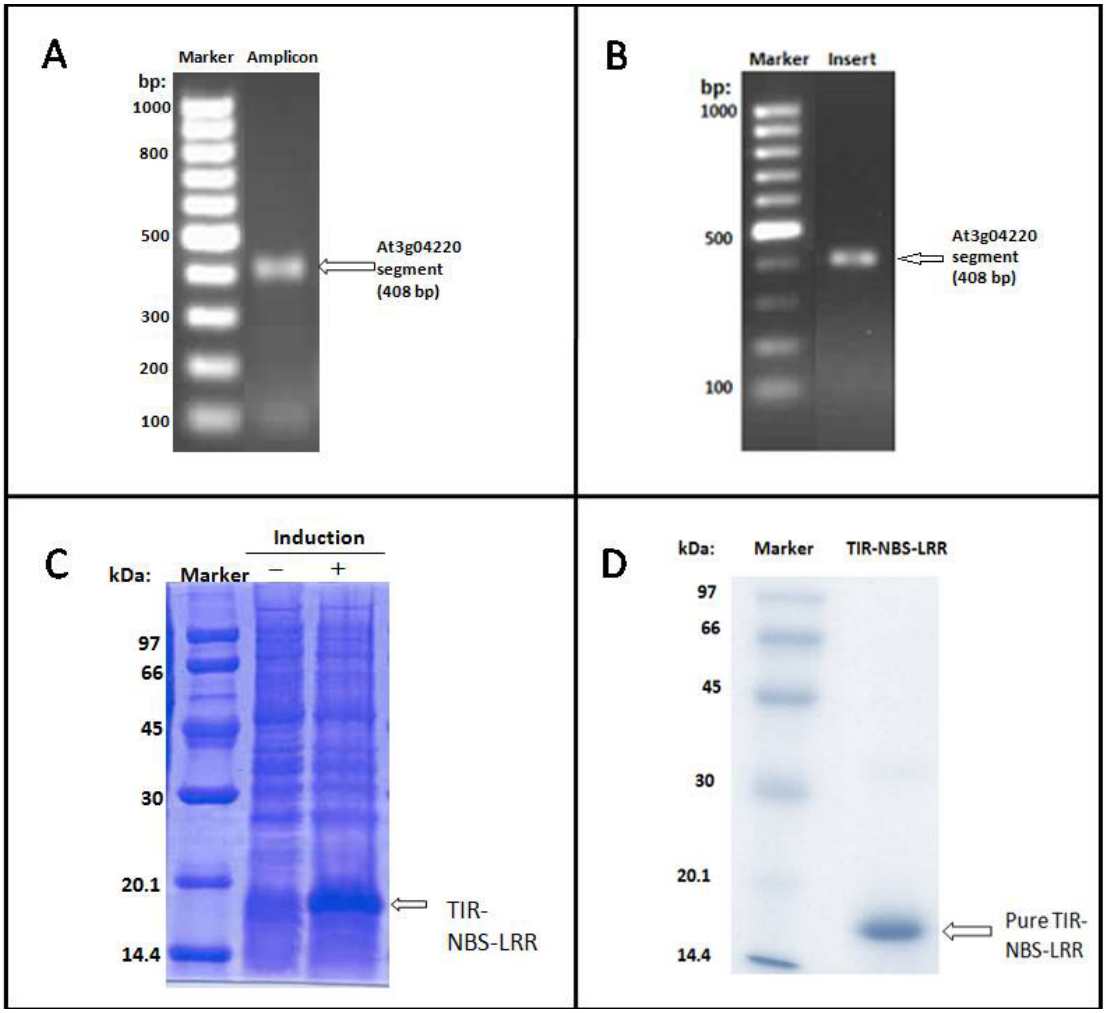

Figure 3.8: Isolation of the At3g04220 gene and the expression and purification of its product. (A) An agarose gel resolution of the partial At3g04220 gene amplified from *A. thaliana* by reverse transcriptase-polymerase chain reaction; where lane 1 represents the 100 bp DNA marker and lane 2 represents the amplified PCR product with the arrow marking the amplified At3g04220 gene fragment. (B) An agarose gel resolution of the confirmatory colony PCR of the At3g04220 gene cloned into the pCR®T7/NT-TOPO® expression vector (Invitrogen, USA) and transformed into *E. coli* BL21 (DE3) pLysS; where lane 1 represents the 100 bp DNA marker (ThermoScientific Ltd, USA) and lane 2 represents the amplified colony PCR product with the arrow marking the expected re-amplified and expected At3g04220 amplicon. (C) An SDS-PAGE of protein fractions expressed in *E. coli* BL21 (DE3) pLysS cells transformed with the pCR®T7/NT-TOPO®-At3g04220 adenylate cyclase fusion construct; where lane 1 represents the low molecular weight marker while (-) and (+) represent protein fractions from the uninduced and induced cultures respectively with the arrow marking the over-expressed TIR-NBS-LRR fusion product. (D) An SDS-PAGE of the purified TIR-NBS-LRR protein; where lane 1 represents the low molecular weight marker (ThermoScientific Ltd, USA) with the arrow marking the purified recombinant fusion product.

3.1.3 Determination of the Endogenous Activity of the Recombinant TIR-NBS-LRR protein

To determine the levels of cAMP generated by the recombinant *E. coli* BL21 (DE3) pLysS harbouring the partial At3g04220 gene under different growth conditions, the cells were cultured until their OD_{600} was 0.5. One portion, the control, was treated with 1 mM IPTG only whilst the second served as the control (Figure 3.9A), the third portion was treated with both 1 mM IPTG and 100 µM forskolin while the last portion was treated with 1 mM IPTG and 100 µM dideoxyadenosine (Figure 3.9B). The generated cAMP was then extracted from the cells and measured by a cAMP-specific enzyme immunoassay kit (Catalogue Number CA201, Sigma, Missouri, USA) based on the acetylation protocol.

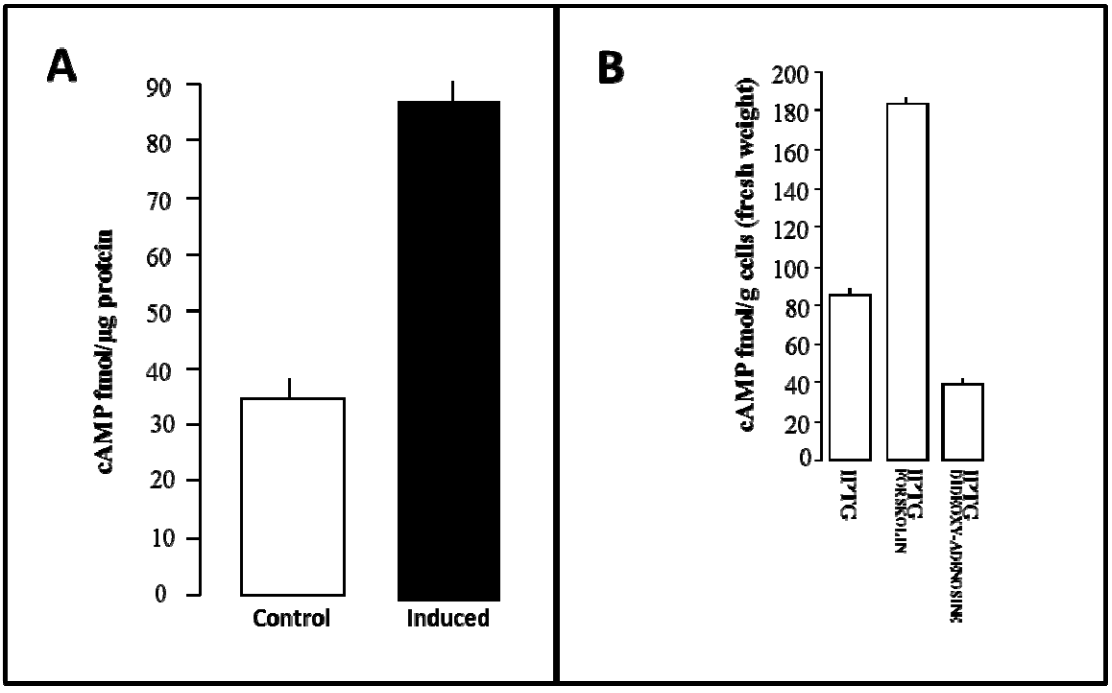

Figure 3.9: Determination of the endogenous adenylate cyclase activity of the recombinant TIR-NBS-LRR protein. **(A)** cAMP levels generated by uninduced (control) and induced *E. coli* BL21 (DE3) pLysS cells harbouring the partial At3g04220 gene. **(B)** cAMP levels generated by induced recombinant cell cultures in the presence of either forskolin or dideoxyadenosine. All cAMP levels were determined using the cAMP Enzyme Immunoassaying system (Catalogue Number CA201, Sigma, Missouri, USA) where error bars represent the standard errors of the means (n=3)

3.1.4 Determination of the *In vitro* Activity of the Recombinant TIR-NBS-LRR Protein

In order to determine the activity of the recombinant protein *in vitro*, the TIR-NBS-LRR protein was expressed by inducing the transformed *E. coli* BL21 (DE3) pLysS with 1 mM IPTG at OD_{600} = 0.5. The expressed protein was then purified on a Ni-NTA affinity matrix. Protein activity was assessed by adding 25 µg purified recombinant TIR-NBS-LRR protein into a reaction system containing 50 mM Tris HCl pH 8.0, 2 mM IBMX, 5 mM Mg^{2+} and 1 mM ATP followed by an incubation at room temperature for 20 minutes. The generated cAMP was then measured by a cAMP-specific enzyme immunoassay kit (Catalogue Number CA201, Sigma, Missouri, USA) based on the acetylation protocol. The effects of 5 mM Mn^{2+}, 100 µM Ca^{2+}, 5 mM GTP and 50 mM CO_3^{2-} as additives to the reaction were also assessed and determined with the same assaying system (Figure 3.10).

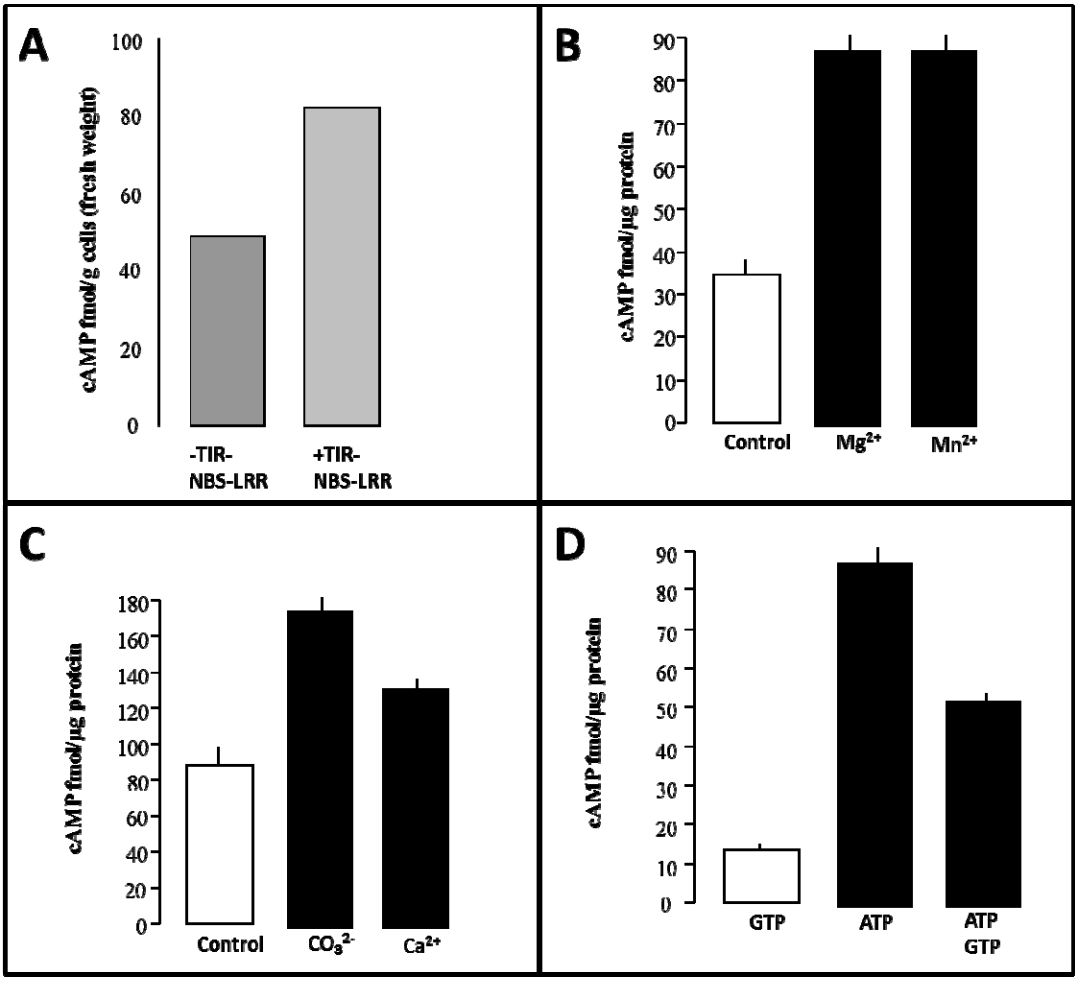

Figure 3.10: Determination of the *in vitro* activity of the recombinant TIR-NBS-LRR protein. A reaction mixture containing 25 µg of the purified recombinant TIR-NBS-LRR adenylate cyclase protein, 50 mM Tris HCl pH 8.0, 2 mM IBMX, 5 mM Mg^{2+}, 1 mM ATP and/or in the presence of other additives was incubated at room temperature for 20 minutes. The generated cAMP was then measured by a cAMP-specific enzyme immunoassay kit (Catalogue Number CA201, Sigma, Missouri, USA) based on the acetylation protocol. **(A)** cAMP levels generated in the absence of the protein (-TIR-NBS-LRR) and in the presence of the protein (+TIR-NBS-LRR). **(B)** cAMP levels generated with the purified recombinant TIR-NBS-LRR in the presence of magnesium or manganese. **(C)** cAMP levels generated with the purified recombinant TIR-NBS-LRR in the presence of carbonate or calcium ions. **(D)** cAMP levels generated with the purified recombinant TIR-NBS-LRR in the presence of either ATP or GTP or ATP and GTP. All error bars represent the standard errors of the means from triplicate assays.

3.1.5 Determination of the *In vivo* Activity of the Recombinant TIR-NBS-LRR Protein

The activity of the recombinant TIR-NBS-LRR protein *in vivo* was tested by assessing the ability of the TIR-NBS-LRR protein to convert the *E. coli cya*A SP850 mutant cells into wild types as a result of their transformation by the pCR®T7/NT-TOPO®-partial-At3g04220 expression construct. The outcome was visually assessed from their phenotypic change on MacConkey agar (Figure 3.11) whereby the white/yellowish colour of mutant cells may change to the magenta/deep purple colour of wild type cells.

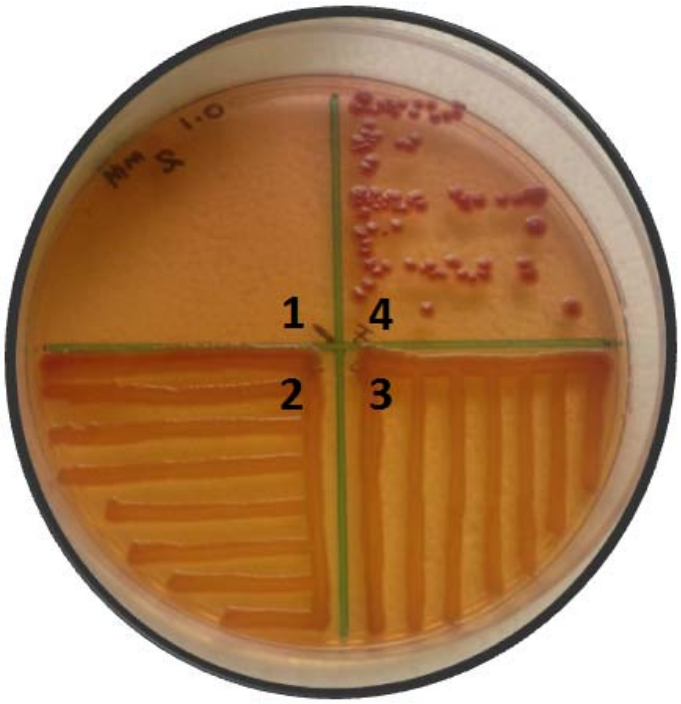

Figure 3.11: Determination of the *in vivo* activity of the recombinant TIR-NBS-LRR protein by a complementation test. Section 1 of the plate contains no cells, section 2 contains non-transformed mutant cells, section 3 contains the mutant cells transformed with the pCR®T7/NT-TOPO® empty vector while section 4 contains the mutant cells transformed with the pCR®T7/NT-TOPO®-At3g04220 expression fusion construct. Cells in sections 2 and 3 are both non-lactose fermenters and produce white or yellowish colonies. Cells in section 4 have picked a magenta/deep purple phenotype signifying a lactose-fermenting phenotype.

3.2 DISCUSSION

3.2.1. Isolation and Amplification of the At3g04220 Gene

This study was set out to address some of the concerns that have been raised in the academic literature with regard to adenylate cyclases in higher plants. Ma and Berkowitz (2007) were concerned that no gene encoding a plant leaf adenylate cyclase had yet been identified or cloned. Moutinho *et al.* (2001) noted that polymorphism is high in the adenylate cyclase family and homologies between bacteria, fungi, and animal sequences are restrained to short motifs; but the abundance of adenylate cyclase isoforms, from prokaryotes to eukaryotes, contrasts with the apparent poverty of adenylate cyclases in plant cells. This led to the suggestion that signal transduction components have diverged considerably, and identification plant adenylate cyclases will not come readily from sequence comparison with animal genes alone.

Significantly and in 2010, Gehring was able to modify a 14-amino acid motif with the capacity for GTP binding and guanylate cyclase activity (deduced from an alignment of conserved and functionally assigned amino acids in the catalytic centre of annotated guanylate cyclases from lower and higher eukaryotes) to a 14-amino acid motif with specificity for ATP-binding and putative adenylate cyclase catalytic activity. A BLAST search of the Arabidopsis genome using this motif managed to identify the TIR-NBS-LRR protein encoded by the At3g04220 gene as a potential and putative adenylate cyclase.

TIR-NBS-LRRs are plant disease resistance proteins which are reported to be involved in cAMP-mediated signal transduction (Vidhyasekaran, 2007). The close relationship between adenylate cyclase activity and stress signaling in plants has been suggested because plant

resistance responses to pathogenic fungi and bacteria often evoke a rapid transient increase in cAMP (Moutinho, 2001). It is unclear how TIR-NBS-LRR is regulated, or how its perception of pathogens could be translated into a rise in cAMP. A possible mechanism for translation of pathogen perception by the TIR-NBS-LRR into increases in cAMP levels could be through G-protein signaling (Ma *et al*., 2009). For this reason, it is important that a determination of the exact physiological role of TIR-NBS-LRR in plant disease resistance be done. However, before this can be accomplished, the mechanism by which cAMP is produced in TIR-NBS-LRR's signaling events needs to be explored. Considering that TIR-NBS-LRR has been implicated as possibly harbouring an adenylate cyclase catalytic centre (Gehring, 2010) and that the only experimentally confirmed higher plant adenylate cyclase, a PSiP protein from *Z. mays*, also belongs to the TIR-NBS-LRR family (Moutinho *et al.,* 2001), it was important that we determine if TIR-NBS-LRR truly does possess adenylate cyclase activity.

Hence, we set out to isolate and clone the At3g04220 gene, and then express and purify its recombinant product, the TIR-NBS-LRR protein fragment containing the adenylate cyclase domain. According to The Arabidopsis Information Resource (TAIR), the full-length genomic sequence of the At3g04220 gene is 3071 nucleotides. However, the same source reveals that the the full-length copy DNA of this particular gene is 2604 nucleotides long. This meant that At3g04220 contains exons and introns (Figure 3.2), whereby the introns are excised from the genomic sequence during transcription to ensure translation of a functional transcript. Essentially, the functional gene product of At3g04220 has an amino acid sequence length of 867, which corresponds to the cDNA sequence. For this reason, the amplification of the At3g04220 gene segment in this study was done using its cDNA as template in a reverse-transcriptase PCR system to produce a functional amplicon which lacked introns (Figure 3.8A). Hence, the

sequence-specific primers were specifically manually designed to amplify from the At3g04220 cDNA (Figure 2,3).

Various evidences have shown that activation of enzymatic active sites is dependent on the conformation of protein's tertiary structure and this conformation is dependent upon the interactions of the different amino acids in the primary structure (Branden and Tooze, 1998). Therefore, the two primers were designed to amplify between positions 1 and 342 of the At3g04220 gene (Figure 2.2) and in order to flank the adenylate cyclase catalytic centre. This primer design was aimed at preserving the adenylate cyclase activity of the truncated TIR-NBS-LRR protein product of the amplified At3g04220 gene segment by ensuring the presence of 50 amino acids sequences flanking the catalytic centre on both the N- and C-termini (Figure 2.1). This therefore further ensured preservation of the primary protein structure necessary for activation of the active site into the correct conformation and particularly, for effective ATP binding and cyclisation. Extra care was also taken to ensure that the forward primer carried the *Bam* HI restriction site and the reverse primer carrying the *Eco* RI restriction site that were both complementary to those of the pCR®T7/NT-TOPO® expression vector (Invitrogen, Carlsbad, USA) into which the amplified gene insert was subsequently going to be cloned. These particular restriction sites were chosen because they are not present within the cloning segment of At3g04220 gene, and thus preventing the possibility of producing an undesirable and non-functional truncated protein.

The sequence specific primers were then used to amplify and isolate the targeted 408 bp At3g04220 gene fragment (Figure 3.8A). Because the pCR®T7/NT®-TOPO plasmid carries a selectable marker in the form of the ampicillin resistance (Amp^R) gene, it enabled the use of

selective pressure in selecting both transformants and recombinants. The At3g04220 gene was successfully ligated into the pCR®T7/NT®-TOPO plasmid to form a recombinant pCR®T7/NT®-TOPO-At3g04220 expression construct.

3.2.2 Expression and Purification of the Recombinant TIR-NBS-LRR Protein

The pCR®T7/NT®-TOPO-At3g04220 expression construct was successfully transformed into the expression host of choice, *E. coli* BL21 (DE3) pLysS, to facilitate expression and purirfication of the recombinant TIR-NBS-LRR adenylate cyclase. Our chief reason for expressing and purifying TIR-NBS-LRR adenylate cyclase from the recombinant expression host is that *A. thaliana*, the natural source, contains such minute quantities of the protein that purification directly from the plant would have been laborious, time-consuming and possibly unfruitful. We therefore needed an expression system that would produce TIR-NBS-LRR adenylate cyclase in sufficiently high quantities and purity to allow for activity assaying. A prokaryotic system was then chosen because of the ability of prokaryotic organisms to grow rapidly and at high density on inexpensive substrates. In particular, *E coli* was the most attractive heterologous expression systems because of its well-characterised genetics and its ability maintain high plasmid copy numbers (Baneyx, 1999).

The choice of the expression host for this study was guided by our need to enable manipulation of pCR®T7/NT®-TOPO's *lac* operon with regard to full expression of the recombinant TIR-NBS-LRR adenylate cyclase and prevention of leaky expression of the At3g04220 gene insert. In this study, we induced over-expression of TIR-NBS-LRR adenylate cyclase using 1 mM IPTG

at OD_{600} of 0.5 of the recombinant cell cultures and in accordance with the protocol of Berrow *et al.* (2006). The expression yielded a recombinant His-tagged fusion protein with the correct predicted molecular weight of 17.64 kDa (Figure 3.8C) and this protein was then purified on a nickel-nitriloacetic matrix (Figure 3.8D).

One disadvantage of expressing heterologous proteins in *E. coli* is that recombinant proteins are frequently expressed as inclusion bodies, which are insoluble aggregated folding intermediates. This necessitates testing for the solubility of the recombinant protein. However, as expected following the *in silico* prediction of 91.3% solubility probability of the recombinant fusion protein (Harrison, 2000), the TIR-NBS-LRR was expressed in the soluble fraction. Hence we were able to avoid the protein solubilisation and refolding process which is a common purification strategy for recombinant proteins which are expressed in inclusion bodies (Harrison, 2000; Stevens, 2000).

3.2.3 Endogenous and *In vitro* Determination of the Activity of the Recombinant TIR-NBS-LRR Protein

In order to determine whether TIR-NBS-LRR is, in fact, an adenylate cyclase, its endogenous and *in vitro* activity was assessed using a cAMP-specific enzyme immunoassay system. To assess whether the recombinant TIR-NBS-LRR protein could possibly contribute to an increase of these intracellular cAMP levels, endogenous activity assay was conducted to determine the levels of cAMP produced within the expression host system both with and without cell induction and in the presence of either 100 μM forskolin or 100 μM dideoxyadenosine. In this assay,

IBMX was used to inhibit phosphodiesterases (Nicholson *et al.,* 1991) which are capable of degrading cAMP. Although the use of IBMX concentrations of 0.5 mM and 1 mM has been documented, this study used 2 mM IBMX and according to Kwezi *et al.* (2007).

The induction of the recombinant cells with 1 mM IPTG resulted in an increase in cAMP generation by over 50 percent as compared to the uninduced recombinant cells (Figure 3.9A). This result is comparable to a previous study where treatment of a pollen-specific putative adenylate cyclase from *Agapanthus umbellatus* (*Liliaceae*) with 1 mM IPTG increased the cAMP levels by a factor of 3 (Malho and Moutinho, 2001). It is important to note that the proteins from the uninduced recombinant cells did produce cAMP, which is attributable to the expression host's own adenylate cyclase/s as well as basal expression of TIR-NBS-LRR adenylate cyclase. However, specific induction of the TIR-NBS-LRR adenylate cyclase protein resulted in over-expression of this particular protein, thus availing more adenylate cyclase active sites and hence, increasing the production of cAMP.

Treatment with 100 µM forskolin resulted in at least a two-fold increase in cAMP production by the recombinant TIR-NBS-LRR adenylate cyclase (Figure 3.9B), thus showing that TIR-NBS-LRR's adenylate cyclase biological activity is indeed enhanced by forskolin. This finding is significant because forskolin is an inducer of intracellular cAMP (Nabaneeta *et al.*, 2004) that specifically was shown to activate adenylate cyclases (Laurenza *et al.*, 1989) in broken cell preparations, membranes and intact cells (Seamon *et al.*, 1981). It has also been shown that 25 mM forskolin causes a 35-fold increase in cAMP in rat cerebral cortical slices, while a low concentration of 1 mM augments the response of cAMP-dependent hormones (Seamon *et al.,* 1981) apparently through direct activation of the enzyme and facilitation of modulation of

enzyme activity. It is important to note that the minute amount of forskolin used in this study was still able to intensify TIR-NBS-LRR's adenylate cyclase activity (Moutinho *et al.,* 2001) even though the use of much higher forskolin concentrations with similar results has been documented (Seamon *et al.,* 1981).

In this study, the treatment of recombinant cells with 25 µm dideoxyadenosine resulted in a decrease of cAMP generation by over 50 percent (Figure 3.1B), meaning that the dideoxyadenosine could inhibit the adenylate cyclase activity of TIR-NBS-LRR adenylate cyclase. Dideoxyadenosine is a potent inhibitor of adenylate cyclases (Désaubry *et al.,* 1996) which leads to a decrease in cAMP production. Fain and Shepherd (1977) found that 10 µM dideoxyadenosine was a potent inhibitor of cAMP accumulation by intact rat liver cells. It has been reported that 2`, 5`-dideoxyadenosine is more potent than adenosine in inhibiting the activation of adenylate cyclase activity at concentrations of up to 73 µM (Fain *et al.*, 1972), and it operates through a P site-mediated inhibition of adenylate cyclase (Johnson *et al.,* 1989). Moreover, the application of 100 µM of dideoxyadenosine to growing pollen tubes transiently caused a temporary growth arrest accompanied by a reduction of cAMP concentration by a factor of 1.8 (Moutinho *et al.,* 2001).

Acetylation of cAMP increases enzyme immunoassay sensitivity for cAMP, hence reducing its sensitivity detection level. The cAMP samples were acetylated because the TIR-NBS-LRR adenylate cyclase protein under assay was a truncated version of the whole protein and only producing cAMP at low levels. Furthermore, the cells used for the assay relied on media-supplied nutrients to supply ATP (as opposed to added ATP in the *in vitro* assay), leading to the need for the acetylation strategy to enable detection of low cAMP levels.

The outcomes of the endogenous assay of the activity of TIR-NBS-LRR adenylate cyclase therefore concur with findings in the existing academic literature. However, the endogenous assay was limited in that it only allowed the conclusion that TIR-NBS-LRR adenylate cyclase is either a *bona fide* adenylate cyclase capable of directly converting ATP to cAMP or it is a functional molecule that stimulates other resident adenylate cyclases in the expression host to produce cAMP. This situation necessitated that we conduct an *in vitro* activity assay using TIR-NBS-LRR adenylate cyclase to now determine whether the cAMP was directly produced from the adenylate cyclase activity of TIR-NBS-LRR adenylate cyclase itself. The *in vitro* assay also allowed for molecular characterization whereby we were able to assess the effect of different ions and molecules on TIR-NBS-LRR's adenylate cyclase activity. Hence, TIR-NBS-LRR adenylate cyclase was purified from the recombinant expression host's total protein on a nickel nitriloacetic affinity matrix followed by its assessment for *in vitro* activity.

The findings obtained show that protein extracted from TIR-NBS-LRR adenylate cyclase recombinant cells produced over 25% more cAMP than the protein produced by the non-recombinant cells (Figure 3.10A). Notably, the non-recombinant cells also possess adenylate cyclase activity. However, the transformation with TIR-NBS-LRR adenylate cyclase results in a significant increase in cAMP production, which can be directly attributed to the adenylate cyclase activity of the recombinant TIR-NBS-LRR adenylate cyclase.

From the results of the *in vitro* assay, it appears that magnesium and manganese had the same intensity of stimulatory effect on the adenylate cyclase activity of TIR-NBS-LRR. Treatment with both ions (at a final concentration of 5 mM [according to Kwezi *et al.,* 2007 and Kwezi *et al.,* 2011]) resulted in the production of the same amount of cAMP, which was over 250% higher

than that produced in the control (Figure 3.9B). While it has been confirmed that magnesium is necessary as a co-factor for adenylate cyclase activity (Cohan *et al*., 1982), several studies have shown that adenylate cyclases can also use manganese (Bilodeau and Goeseels, 2003). In *Dictyostelium*, two adenylate cyclases exhibited increased activity in the presence of manganese (Anjard *et al.,* 2001). The results of this assay show that magnesium and manganese function equally to enhance the adenylate cyclase activity of TIR-NBS-LRR adenylate cyclase, and that TIR-NBS-LRR adenylate cyclase exhibits no preference for one over the other as a co-factor for its enzymatic activity. This is in stark contrast to guanylate cyclases, which require and prefer manganese ions over magnesium ions as co-factors (Nathanson, 1977). In fact, adenylate cyclase activity has been shown to increase in a dose-dependent manner in the presence of either ion.

Treatment with carbonate ions increased cAMP production by almost 100 percent (Figure 3.10C). Carbonate ions have been implicated in the activation of adenylate cyclases (Okamura *et al.,* 1990) as functional modulators. This compares favourably with the findings of Garty and Salomon (1987) and Visconti *et al.* (1990) who reported the direct activation of adenylate cyclase by carbonate ions resulting in a four-fold increase in cAMP production. Moreover, Chen *et al*. (2000) reported that carbonate increases cAMP generation in a pH-independent manner. Hence, we find that the adenylate cyclase activity of the TIR-NBS-LRR is directly and favourably modulated by carbonate ions.

Calcium definitely stimulates increased production of cAMP by TIR-NBS-LRR adenylate cyclase, as evidenced by the fact that the calcium-treated protein produced over 50% more cAMP as opposed to the control (Figure 3.10C). This concurs with the literature that free

calcium ions stimulate both adenylate and guanylate cyclase activities, and play an important role in the cellular actions of both cAMP and cGMP (Nathanson, 1977). However, this role is unclear and it has been suggested that calcium regulates cAMP synthesis directly or indirectly (Halls and Cooper, 2011).

The finding that calcium has a stimulatory effect on the adenylate cyclase activity of TIR-NBS-LRR is significant because another leucine-rich repeat protein from *A. thaliana,* AtPepR1, has been reported to have guanylate cylase activity that is simultaneously involved in the Ca^{2+} pathway associated with pathogen defense (Qi *et al.,* 2010). Furthermore, it is noteworthy that cAMP elevation at the infection site has been linked to the initiation of pathogen defense-related cytosolic calcium signaling, implying that cAMP may have a specific role in plant-defense signal cascades (Ma *et al.,* 2009). The parallel occurrence of and requirement for cyclic nucleotide and Ca^{2+} signalling is a recurring theme in defence-related responses (Bindschedler *et al.,* 2001). In addition, a recent study found major gaps in suspected calcium interactions of adenylate cyclases, thus leading to the conclusion that the effects of calcium on individual adenylate cyclases must be clarified (Halls and Cooper, 2011). The possible adenylate cyclase activity of TIR-NBS-LRR thus provides a potential paradigm for linking pathogen perception to calcium signaling and immune response in plants and provides a basis for further analysis of the biological activity of TIR-NBS-LRR adenylate cyclase in terms of cross-talking with calcium.

The substrate specificity of the recombinant TIR-NBS-LRR between ATP and GTP was also assessed by testing its ability to generate cAMP from either of the two substrates. It is noteworthy that GTP exhibited an inhibitory effect on the adenylate cyclase activity of TIR-NBS-LRR. ATP-treated protein produced 8-fold the amount of cAMP produced by GTP-treated

protein. The sample treated with both ATP and GTP produced an intermediate amount of cAMP, which was almost 4-fold as compared to the GTP-treated sample and just over half as compared to the ATP-treated sample (Figure 3.10D). These findings provide evidence for the strict specificity of TIR-NBS-LRR for ATP and the competitive binding to the adenylate cyclase of both the structurally analogous ATP and GTP

Interestingly, there are contrasting views on the effect of GTP on adeylate cyclase activity. While it has been found that adenylate cyclase activity is potentiated by GTP (Krishna *et al.,* 1972; Nathanson, 1977; Seamon *et al.,* 1981), it has been reported that low concentrations of GTP (<30 nM) increase adenylate cyclase activity whereas higher concentrations cause a steady decline in activity (Cooper *et al.,* 2006). This observation is consistent with our finding that 5 mM GTP inhibited the adenylate cyclase activity of TIR-NBS-LRR. Krishna *et al.* (1972), however, were of the opinion that although low concentrations of GTP markedly increase adenylate cyclase enzymatic activity, the GTP does not alter the apparent affinity of the enzyme for ATP.

In plants, adenylate cyclase activity is low and cAMP is barely detectable (Ichikawa *et al.,* 1997). For the *in vitro* assay, it is possible that higher activity would have required co-factors or post-translational modifications which were not present in the reaction mix (Kwezi *et al.,* 2007). However, our findings indicate that IPTG, Mg^{2+}, Mn^{2+}, Co_3^{2-}, Ca^{2+} and GTP have significant effects on the adenylate cyclase catalytic activity of the recombinant TIR-NBS-LRR adenylate cyclase protein.

3.2.4 The *In vivo* Determination of the Activity of TIR-NBS-LRR

While the findings of the *in vitro* activity assay allowed for the conclusion that TIR-NBS-LRR adenylate cyclase is indeed a functional adenylate cyclase, it was considered necessary to to further validate this outcome through a functional complementation test for the *in vivo* activity of TIR-NBS-LRR adenylate cyclase. The complementation test made use of Crystal Violet Neutral Red Bile Lactose Agar, otherwise known as MacConkey Agar (MacConkey, 1905), which is used for the presumptive identification of coliforms, including *E. coli*. The agar selects for enteric bacteria due to the inclusion of highly purified bile salts, and by colour differentiation between lactose- and non-lactose fermenting organisms. Enterococci of the lactose-fermenting phenotype will produce magenta-coloured colonies upon growth on the media.

Wild type *E. coli* is a lactose fermenter but the *cyaA SP850* strain, which lacks adenylate cyclase activity due to a *cya*A deletion mutation, cannot metabolise lactose and produces yellow-orange colonies on MacConkey agar. It has been shown that *E. coli* cells which do not produce cAMP are unable to ferment lactose and produce colourless to orange-coloured colonies on MacConkey agar, whereas cAMP production enables lactose fermentation, thus resulting in growth of magenta-coloured colonies. The *cya*A mutant strain therefore provided a method of confirming the catalytic activity of the putative adenylate cyclase candidate TIR-NBS-LRR by its expression in the *cya*A strain (Tang and Gilman, 1995; Moutinho *et al.,* 2001).

When transformed with the At3g04220 gene, the recombinant *E. coli cya*A SP850 mutants were able to utilize lactose as a result of the activation of the *lac* operon of the pCR®T7/NT-TOPO®-At3g04220 by IPTG and hence, produced magenta-coloured colonies signifying a rescued cAMP-dependent lactose fermentation of the recombinant *cya*A mutant cells harbouring the

At3g04220 gene. This confirmed that TIR-NBS-LRR has the ability to produce cAMP and is therefore, an adenylate cyclase. This *in vivo* assay thus validated the results of the endogenous and the *in vitro* assays, proving that TIR-NBS-LRR possesses adenylate cyclase catalytic activity that is intrinsic to itself.

3.3 CONCLUSIONS

Following on the bioinformatic identification of TIR-NBS-LRR as a putative adenylate cyclase and according to the search motif for the adenylate cyclase catalytic centre, we have successfully cloned, expressed and purified the TIR-NBS-LRR adenylate cyclase protein. Furthermore, the findings of this study show that the TIR-NBS-LRR protein encoded by the At3g04220 gene from *Arabidopsis thaliana* is a functional higher plant adenylate cyclase. TIR-NBS-LRR adenylate cyclase is therefore the second higher plant adenylate cyclase to be experimentally identified after the *Z. mays* pollen protein which was identified in 2001 (Moutinho *et al.*, 2010). Moreover, our molecular characterization of the adenylate cyclase activity of the TIR-NBS-LRR, has shown that it is enhanced by magnesium, manganese, carbonate, calcium and forskolin; while conversely, it is down-regulated by GTP and dideoxyadenosine.

3.4 RECOMMENDATIONS

The outcomes of this study allow for a number of possible and feasible recommendations. Firstly, our experimentally confirmed adenylate cyclase in addition to the known *Z. mays* adenylate cyclase can however, on their own, not account for the number or diversity of all cAMP-dependent responses in higher plants. Interestingly, eight other genes from *A. thaliana*

encode a putative adenylate cyclase domain with the same functionally assigned residues in the catalytic centre as At3g04220 (Gehring, 2010). It is conceivable that other proteins containing the adenylate cyclase search motif may also have catalytic activity, meaning that numerous other plant adenylate cyclases remain to be discovered and must be functionally characterised.

Secondly, it has been shown that adenylate cyclase activity is stimulated by ozone (Roshchina and Roshchina, 2003) while contrasting reports provide evidence for both stimulation and inhibition of adenylate cyclase activity by nitric oxide (Gray and Marshall, 1992; McVey *et al.*, 1999). There is, therefore, a need for further molecular characterization of TIR-NBS-LRR, principally to investigate the effect of ozone and nitric oxide on its adenylate cyclase catalytic activity. The effect of differing concentrations of GTP which was alluded to Section 3.2.3 also needs to be investigated further.

Thirdly, although this study has confirmed the adenylate cyclase catalytic activity of TIR-NBS-LRR endogenously, *in vitro* and *in vivo*, it still remains to be seen whether this protein possesses *in planta* activity. *In vivo* assays of the recombinant TIR-NBS-LRR in *A. thaliana* protoplasts will provide verification of its *in planta* adenylate cyclase catalytic activity.

The TIR-NBS-LRR protein, apart from the ATP-binding adenylate cyclase catalytic centre (amino acids 62-77), has a second ATP-binding and hydrolysis site located in the NBS domain (amino acids 257-398). As opposed to the adenylate cyclase catalytic centre, the NBS ATP-binding site hydrolyses ATP to ADP. Hence, the fourth recommendation is that is important to investigate whether there is crosstalking between these two ATP-binding functions, in terms of up- or down-regulation of the adenylate cyclase activity, or lack thereof.

The implementation of these recommendations will assist in elucidating the exact physiological and biochemical role of TIR-NBS-LRR in cell signal transduction and, particularly, in plant stress response and adaptation.

3.5 FUTURE OUTLOOK

The speculation that the plant adenylate cyclases might be disguised under the broad spectra of large gene families seems likely since Gehring (2010) also identified putative adenylate cyclases in *A. thaliana* from such families as epsins, pentatricopeptides, F-box proteins and linker histone-like proteins. Certainly, the subject of this study, the TIR-NBS-LRR protein, not only belongs to the NBS-LRR plant disease resistance protein family, but also to the Signal Transduction ATPases with Numerous Domains (STAND) family. In fact, one of the first plant disease resistance genes to be cloned, the *RPS2* gene, contains leucine zipper, P loop domains, and leucine-rich repeats, an interaction domain similar to that of a yeast adenylate cyclase (Bent *et al.*, 1994). Moreover, it has been reported that nucleotidyl cyclase domains tend to make multi-functional enzymes ('moonlighting proteins' with dual functions) by combining with other proteins (Meier *et al.,* 2007) and it is possible that TIR-NBS-LRR may be one such 'moonlighting protein' given its multi-functional domain organisation.

It has been shown that membrane-bound receptor guanylate cyclases are multi-domain proteins with an extracellular ligand-binding domain, a membrane-spanning domain, an intracellular domain with homology to protein kinases, and a C-terminally located cyclase domain. As such, they are multi-domain proteins whose associated domains allosterically regulate the activity of

the catalytic domain (Biswas *et al*., 2009). The TIR-NBS-LRR protein under study is one such multi-domain protein, being a membrane-bound receptor having the toll interleukin-like receptor (TIR), the nucleotide binding site (NBS) and the leucine-rich repeat (LRR) domains in the N→C direction respectively. It differs, however, from the previously mentioned guanylate cyclases in that the adenylate cyclase catalytic centre is N-terminally located. Its intracellular LRR domain, like most other LRR sequences, is probably involved in protein-protein interactions while the intracellular NBS domain possesses kinase motifs. We therefore propose that the TIR-NBS-LRR protein may be subject to allosteric regulation, whereby ligand binding in the LRR or NBS domain may result in the activation of the adenylate cyclase domain due to a resultant conformational change.

Furthermore, generally, most active kinase domain-containing proteins possess active adenylate cyclase or unusual nucleotide cyclase domains (Biswas *et al*., 2009). One report on a retinal guanylate cyclase indicates that it has self-phosphorylating activity (Aparicio and Applebury, 1996). This is significant in light of the fact that the NBS domain of the TIR-NBS-LRR protein contains consensus kinase 1a (P-loop), kinase 2 and kinase 3a motifs (Moffett *et al.,* 2002). The proximity of the kinase motifs to the adenylate cyclase catalytic centre suggests allosteric regulation of TIR-NBS-LRR from the NBS domain that can be linked to the regulation of the adenylate cyclase catalytic centre.

This is all the more significant given that the tyrosine residue of TIR-NBS-LRR's adenylate cyclase catalytic centre (amino acid 63) has been experimentally proven to be a phosphorylation site (Engelsberger and Schulze, 2012) and that amino acids 51-72 (including the amino acids 62-72 of the adenylate cyclase catalytic centre) are predicted with a score greater than 0 to be a

phosphorylation hotspot by the PhosPhAt 4.0 Protein Phosphorylation Prediction Server (Heazlewood *et al.,* 2008; Durek *et al.,* 2010). The transduction of a signal often relies on the post-translational modification (PTM) of proteins (Mithoe and Menke, 2011). Although studies have demonstrated that amino acid phosphorylation plays a key role in regulation of plant growth, development, pathogenesis and defense-related signalling, tyrosine phosphorylation, as opposed to serine/threonine phosphorylation, has largely been neglected because a typical protein kinase was not found in plants (Luan, 2002). At the molecular level, tyrosine phosphorylation plays diverse roles including enzyme activation and deactivation in mammals (Jaillais *et al.,* 2011).

Given the above information, is it possible for the kinase sub-domains of the NBS domain to be cAMP-dependent kinases which autophosphorylate the tyrosine at the adenylate cyclase catalytic centre, thus activating this catalytic centre via a positive feedback regulatory process?

Lastly, the work accomplished thus far on the TIR-NBS-LRR adenylate cyclase protein has laid a good foundation for the determination of cAMP-dependent proteomes. Very few downstream targets for cAMP have been identified but they are likely to include membrane transporters, transcription factors and kinases. To date, however, cAMP-dependent kinases have not been found in plants. It has been suggested that cyclic nucleotide-gated channels (CNGCs), a recently identified family of plant ion channels, might be the prime targets of cyclic nucleotides as downstream effectors in plants. In fact, the existence of CNGCs as ligand-gated calcium-permeable channels suggests that they function where calcium signalling pathways and cyclic nucleotide signalling pathways meet, in processes such as plant defence response (Talke *et al.,* 2003). The evident role of CNGCs in pathogen responses might well provide a hint about the

molecular identity of a missing target of plant cyclic nucleotide signals, the protein kinases. While protein kinases have remained obscure in plants, calcium-dependent protein kinases (CDPKs) are known to be encoded by a large gene family (Harmon *et al*., 2001). CDPKs have been shown to be involved in several processes in plant physiology: not only in defence signalling but also in tolerance to environmental stresses such as cold, drought or salinity (Saijo *et al.,* 2000; Romeis *et al.,* 2001).

It has been proposed that integrated signalling pathways of plant CNGCs involve cAMP and Ca^{2+}. This suggests CNGCs to be a prime target for cAMP in plant cells and provides an alternative pathway through which changes in the cytosolic cAMP concentration would lead to changes in the phosphorylation status and thus the activity of proteins (Talke *et al.,* 2003). Hence, it is conceivable that the cAMP generated by TIR-NBS-LRR has one or a number of cAMP-gated channels as its target/s; and that CDPKs are a part of its downstream signalling pathway. This is even more plausible if the co-expression patterns of At3g04220 are taken into account, whereby the gene is said to be co-expressed with a CNGC-encoding gene (At3g17690) alongside various defense response-encoding genes (At3g23250, At1g80820, At5g22530, At5g38340, At5g03800 and At5g38350) (Biological Open Linked Database, 2012).

An elucidation of these proteomes will significantly increase our understanding of signal transduction in plants and open up new avenues for improvement of food crops and increase of agricultural yields.

REFERENCES

Ade J, DeYoung BJ, Goldstein C and Innes RW. **Indirect activation of a plant nucleotide binding site-leucine-rich repeat protein by a bacterial protease**. *Proceedings of the National Academy of Sciences* 2007, **104**(7):2531-2536

Al-Bader AA, Rao PN and Orengo A. **The relationship of cAMP levels and the rate of pool labeling of cAMP and related bases, nucleosides and nucleotides to the HeLa cell cycle.** *Experimental Cell Research* 1976, **103**(1): 47-54

Ameline-Torregrosa C, Wang B, O'Bleness MS, Deshpande S, Zhu H, Roe B, Young NB and Cannon SB. **Identification and Characterization of Nucleotide-Binding Site-Leucine-Rich Repeat Genes in the Model Plant *Medicago truncatula*.** *Plant Physiology January* 2008, **146**(1): 5-21

Anjard C, Söderbom F and Loius WF. **Requirements for adenylyl cyclases in the development of *Dictyostelium*.** *Development* 2001, **128**: 3649-3654

Aparicio JG and Applebury ML. **The photoreceptor guanylate cyclase is an autophosphorylating protein kinase.** *Journal of Biological Chemistry* 1996, **271:** 27083–27089

Assmann S. **Cyclic AMP as a second messenger in higher plants (Status and future prospects).** *Plant Physiology* 1995, **108**(3):885-889

Atkinson NJ and Urwin PE. **The interaction of plant biotic and abiotic stresses: from genes to the field.** *Journal of Experimental Botany* 2012, **10**: 1093

Baneyx F. **Recombinant expression in *Escherichia coli*.** *Current Opinion in Biology* 1999, **10**: 411-421

Belkhadir Y, Subramaniam R and Dangl JL. **Plant disease resistance protein signalling: NBS-LRR proteins and their partners.** *Current Opinion in Plant Biology* 2004, **7**:391-399

Bent AF. **Plant disease resistance genes: Function meets structure**. *The Plant Cell* 1996, **8**: 1757-1771

Bernoux M, Ellis JG and Dodds PN. **New insights in plant immunity signaling activation**. *Current Opinion in Plant Biology* 2001, **14**: 512-518

Berrow NS, Büssow K, Coutard B, Diprose J, Ekberg M, Folkers GE, Levy N, Lieu V, Owens RJ, Peleg Y, Pinaglia C, Qeuvillon-Cheruel S, Salim L, Scheich C, Vincentelli R and Busso D. **Recombinant protein expression and solubility screening in *Escherichia coli*: a comparative study.** *Biological Crystallography* 2006, **62**(10): 1218-1226

Bilodeau S and Goeseels. **Manganese inhibits spontaneous nuclear maturation via the cAMP/Protein Kinase A pathway in bovine cumutus-enclosed oocytes.** *Journal of Animal and Veterinary Advances* 2003, **2**(1): 12-21

Bindschedler LV, Minibayeva F, Gardner SL, Gerrish C, Davies DR and Bolwell GP. **Early signalling events in the apoplastic oxidative burst in suspension cultured French bean cells involve cAMP and Ca^{2+}.** *New Phytologist* 2001, **151**: 185–194

Biswas KH, Shenoy AR, Dutta A and Visweswariah SS. **The evolution of guanylyl cyclases as multidomain proteins: Conserved features of kinase-cyclase domian fusions.** *Journal of Molecular Evolution* 2009, **68**: 587-602

Burch-Smith TM and Dinesh-Kumar SP. **The functions of plant TIR domains.** *Science Signaling* 2007, **2007**(401): 46

Cannon SB, Zhu H, Baumgarten AM, Spangler R, May G, Cook DR and Young ND. **Diversity, distribution, and ancient taxonomic relationships within the TIR and non-TIR-NBS-LRR resistance gene subfamilies**. *Journal of Molecular Evolution* 2002, **54**: 548-562

Chadwick CM and Garrod DR. **Plant receptor-ligand interactions.** *Hormones, receptors and cellular interactions in plants.* Intercellular Communication Volume 1. Cambridge University Press 1986. United Kingdom. Pp375

Chen Q, Han Z, Jiang H, Dacheng T and Yang S. **Strong positive selection drives rapid diversification of *R*-genes in Arabidopsis relatives**. *Journal of Molecular Evolution* 2010, **70**: 137-148

Chen Y, Cann MJ, Litvin TN, Iourgenko V, Sinclair ML, Levin LR and Buck J. **Soluble adenylyl cyclase as an evolutionary conserved bicarbonate sensor.** *Science* 2000, **289**: 625

Cohan BW, Singer FR and Rude RK. **End-Organ Response to Adrenocorticotropin, Thyrotropin, Gonadotropin-Releasing Hormone, and Glucagon in Hypocalcemic Magnesium Deficient Patients.** *Journal of Clinical Endocrinology and Metabolism* 1982, **54**: 975-979;

Cooper DMF, Londos C, Gill DL and Rodbell M. **Opiate receptor-mediated inhibition of adenylate cyclase in rat striatal plasma membranes.** *Journal of Neurochemistry* 2006, **38(**4): 1164-1167

Denby K and Gehring C. **Engineering drought and salinity tolerance in plants: lessons from genome-wide expression profiling in Arabidopsis.** *Trends in Biotechnology* 2005, **23**(11): 547-552

Désaubry L, Shoshani I and Johnson RA. **2′5′-Dideoxyadenosine 3′-polyphosphates are potent inhibitors of adenylyl cyclases.** *The Journal of Biological Chemistry* 1996, **271**: 2380-2382

DeYoung BJ and Innes RW. **Plant NBS-LRR proteins in pathogen sensing and host defence.** *Nature Immunology* 2006, **7**: 1243-1249

Durek P, Schmidt R, Heazlewood JL, Jones A, Maclean D, Nagel A, Kersten B and Schulze WX, **PhosPhAt: The *Arabidopsis thaliana* phosphorylation site database. An update.** *Nucleic Acids Research* 2010, **38**: D828-D834

Edman P. In *Protein Sequence Determination* (Second Edition). Needleman SB (Ed). Springer-Verlag 1975. Germany. Pp393

Eitas TK and Dangl JL. **NB-LRR proteins: pairs, pieces, perception, partners and pathways**. *Current Opinion in Plant Biology* 2010, **13**: 472-477

Engelsberger, W. R. and Schulze, W. X. **Nitrate and ammonium lead to distinct global dynamic phosphorylation patterns when resupplied to nitrogen-starved *Arabidopsis* seedlings.** *The Plant Journal* 2012, **69**(6): 978–995

Enkhbayar P, Kamiya M, Osaki M, Matsumoto T and Matsushima N. **Structural principles of leucine-rich repeat (LRR) proteins.** *Proteins* 2004, **54**:394-403

Ensembl Genome Browser. 2012. Available at http://plants.ensembl.org/Arabidopsis_thaliana/Gene/Summary?g=AT3G04220;r=3:1109118-1112188;t=AT3G04220.1 on 10/09/2012 at 1543hrs

Faigon-Soverna A, Harmon FG, Storani L *et al*. **A constitutive shade-avoidance mutant implicates TIR-NBS-LRR proteins in *Arabidopsis* photomorphogenic development.** *The Plant Cell* 2006, **18**(11): 2919-2928

Fain JN and Shepherd RE. **Adenosine cyclic AMP metabolism, and glycogenolysis in rat liver cells.** *The Journal of Biological Chemistry* 1977, **252**(22): 8066-8070

Fain JN. Pointer RH and Ward WF. **Effects of adenosine nucleosides on adenylate cyclase, phosphodiesterase, cyclic adenosine monophosphate accumulation, and lipolysis in fat cells.** *The Journal of Biological Chemistry* 1972, **247**: 6866-6872

Gachomo EW. Shonukan OO and Kotchoni SO. **The molecular initiation and subsequent acquisition of disease resistance in plants.** *African Journal of Biotechnology* 2003, **2**(2): 26-32

Garty NB and Salomon Y. **Stimulation of partially purified adenylate cyclase from bull sperm by bicarbonate.** *Federation of European Biochemical Societies* 1987, **218**(1): 148-152

Gassmann W, Hinsch ME and Staskawicz BJ. **The Arabidopsis RPS4 bacterial-resistance gene is a member of the TIR-NBS-LRR family of disease-resistance genes.** *The Plant Journal* 1999, **20**(3): 265-277

Gasumov KG, Shichijo C, Bayramov SM and Hashimoto T. **Membrane and soluble fractions of adenylyl cyclase from *Sorghum bicolor* seedlings positively react to the action of red and far red lights.** *Internet Photochemistry and Photobiology.* Available at http://www.photobiology.com/index.htm on 14/03/2013 at 0852hrs.

Geffroy V, Macadre C, David P, Pedrosa-Harand A, Sevignac M, Dauga C and Langin T. **Molecular analysis of a large subtelomeric NBS-LRR family in two representative genotypes of the major gene pools of *Phaseolus vulgaris*.** *Genetics* 2008, **10**: 1534

Gehring C. **Adenylyl cyclases and cAMP in plant signaling – past and present.** *Cell Communication and Signalling*2010, **8**: 15

Grant JJ, Chini A, Basu D and Loake GJ. **Targeted activation tagging of the Arabidopsis NBS-LRR gene, ADR1, conveys resistance to virulent pathogens.** *MPMI* 2003, **16**(8): 669-680

Gray DW and Marshall I. **Human α-calcitonin gene-related peptide stimulates adenylate cyclase and guanylate cyclase and relaxes rat thoracic aorta by releasing bitric oxide.** *British Journal of Pharmacology* 1992, **107**: 691-696

Gururani MA, Venkatesh J, Upadhyaya CP, Nookaraju A, Pandey SK and Park SW. **Plant disease resistance genes: Current status and future directions**. *Physiological and Molecular Plant Pathology* 2012, **78**: 51-65

Halls ML and Cooper DMF. **Regulation by Ca2+-signaling pathways of adenylyl cyclases.** *Cold Spring Harbor Perspectives in Biology* 2011, **3**: a004143

Hanahan D. **Studies on transformation of *Escherichia coli* with plasmids.** *Journal of Molecular Biology* 1983, **166**(4): 557-580

Harmon AC, Gribskov M, Gubrium E and Harper JF. **The CDPK superfamily of protein kinases.** *New Phytologist* 2001, **151**: 175–183

Harrison RG. **Expression of soluble heterologous proteins via fusion with NusA protein kinases.** *New Phytologist* 2001, **151**: 175-183

Heazlewood JL, Durek P, Hummel J, Selbig J, Weckwerth W, Walther D and Schulze WX. PhosPhAt: **A Database of phosphorylation sites in *Arabidopsis thaliana* and a plant specific phosphorylation site predictor.** *Nucleic Acids Research* 2008, **36**: D1015-D1021

Hintermann R and Parish RW. **Determination of adenylate cyclase activity in a variety of organisms: Evidence against the occurrence of the enzyme in higher plants.** *Planta* 1979, **146**(4): 459-461

Hussain K, Nisar MF, Majeed A, Nawaz K, Bhatti KH, Afghan S, Shahazad A and Zia-ul-Hussnian S. **What molecular mechanism is adapted by plants during salt stress tolerance?** *African Journal of Biotechnology* 2010, **9**(4): 416-422

Ichikawa T, Suzuki Y, Czaja I, Schommer C, LeBnick A, Schell J and Walden R. **Identification and role of adenylyl cyclase in auxin signaling in higher plants.** *Nature* 1997, **390**: 698-701

Jaillais Y, Hothorn M, Belkhadir Y, Dabi T, Nimchuk ZL, Meyerowitz EM and Chory J. **Tyrosine phosphorylation controls brassinosteroid receptor activation by triggering membrane release of its kinase inhibitor.** *Genes and Development* 2011, **25**: 232-237

Johnson RA, Yeung SM, Stübner D, Bushfield M and Shoshanii. **Cation and structural requirements for P site-mediated inhibition of adenylate cyclase.** *Molecular Pharmacology* 1989, **35**(5): 681-688

Jones JDG. **Putting knowledge of plant disease resistance genes to work**. *Current Opinion in Plant Biology* 2001, **4**: 281-287

Kajava AV, Kobe B. **Asessment of the ability to model proteins with leucine-rich repeats in light of the latest structural information**. *Protein Sci* 2002, **11**:1082-1090

Kelley LA and Sternberg MJE. **Protein structure prediction on the web: a case study using the Phyre server**. *Nature Protocols* 2009, **4**:363–371.

Kobe B, Kajava AV. **The leucine-rich repeat as a protein recognition motif**. *Current Opinion in Structural Biology* 2001, **11**:725-732

Krishna G, Harwood JP, Barber AJ and Jamieson GA. **Requirement for guanosine triphosphate in the prostaglandin activation of adenylate cyclase of platelet membranes.** *Journal of Biological Chemistry* 1972, **247**(7): 2253-2254

Kwezi L, Meier S, Mungur L, Ruzvidzo O, Irving H and Gehring C. **The *Arabidopsis thaliana* Brassinosteroid Receptor (AtBRI1) contains a domain that functions as a guanylyl cyclase *in vitro*.** *PLoS ONE* 2007, **2**(5): e449

Kwezi L, Ruzvidzo O, Wheeler JI, Govender K, Iacuone S, Thompson PE, Gehring C and Irving HR. **The Phytosulfokine (PSK) Receptor is capable of guanylate cyclase activity and**

enabling cyclic GMP-dependent signaling in plants. *The Journal of Biological Chemistry* 2011, **286**(25): 22580-22588

Laurenza A, Sutkowski EM and Seamon KB. **Forskolin: a specific stimulator of adenylyl cyclase or a diterpene with multiple sites of action?** *Trends in Pharmacological Science* 1989, **10**(11): 442-447

Li W, Luan S, Schreiber SL and Assmann SM. **Cyclic AMP stimulates K^+ channel activity in mesophyll cells of *Vicia faba* L.** *Plant Physiology* 1994, **106**(3): 957–961

Logemann J, Schell J and Willmitzer L**. Improved method for the isolation of RNA from plant tissues.** *Analytical Biochemistry* 1987, **163**(1): 16

Lomovatskaya L, Anatoliy R and Nadejda F. **Plant adenylate cyclases.** *Journal of Receptors and Signal Transduction* 2008, **28**(6): 531-542

Lozano R, Ponce O, Ramirez M, Mostajo N and Orjeda G**. Genome-wide identification and mapping of NBS-encoding genes in *Solanum tuberosum* Group Phureja.** *PLoS ONE* 2012, **7**(4):e34775

Luan S. **Tyrosine phosphorylation in plant cell signaling.** *Proceedings of the National Academy of Science* 2002, **99**(18): 11567-1159

Ludidi N and Gehring C. **Identification of a novel protein with guanylyl cyclase activity in *Arabidopsis thaliana*.** *The Journal of Biological Chemistry* 2003, **278**: 6490-6494

Ma S, Gong Q and Bohnert HJ. **Dissecting salt stress pathways.** *Journal of Experimental Botany* 2006, **57**(5): 1097-1107

Ma W and Berkowitz GA. **The grateful dead: calcium and cell death in plant innate immunity**. *Cellular Microbiology* 2007, **9**(11): 2571-2585

Ma W, Qi Z, Smigel A, Walker RK, Verma R and Berkowitz GA. **Ca^{2+}, cAMP, and transduction of non-self perception during plant immune responses.** *Proceedings of the National Academy of Science* 2009, **106**: 20995-21000

MacConkey A. **Lactose-fermenting bacteria in faeces.** *Journal of Hygiene* 1905, **5**(3): 333-379

Malho R and Moutinho A. **A cAMP pathway in pollen tube growth and reorientation.** *Cell Biology of Plant and Fungal Tip Growth.* Geitmann A *et al*. (Eds). 2001. IOS Press. Netherlands.

McDowell JM and Woffenden BJ. **Plant disease resistance genes: recent insights and potential applications.** *TRENDS in Biotechnology* 2003, **21**(4) 178-183

McHale L, Tan X, Koehl P and Michelmore RW. **Plant NBS-LRR proteins: adaptable guards.** *Genome Biology*. 2006, **7**:212

McVey M, Hill J, Howlett A and Klein C. **Adenylyl cyclase, a coincidence detector for nitric oxide**. *The Journal of Biological Chemistry* 1999, **274:** 18887-18892

Meier S, Ruzvidzo O, Morse M, Donaldson L, Kwezi L and Gehring C. **The Arabidopsis *Wall Associated Kinase-Like 10* Gene Encodes a Functional GuanylylCyclase and Is Co-Expressed with Pathogen Defense Related Genes**. *PLoS ONE* 2010, **5**(1): e890

Michelmore R. **Genomic approaches to plant disease resistance.** *Current Opinion in Plant Biology* 2000, **3**: 125-131

Mithoe SC and Menke FLH. **Phosphoproteomics perspective on plant signal transduction and tyrosine phosphorylation.** *Phytochemistry* 2011, **72**(10): 997-1006

Moffett P, Farnham G, Peart J and Baulcombe DC**. Interaction between domains of a plant NBS-LRR protein in disease resistance-related cell death.** *The EMBO Journal* 2002, **21**(17): 4511-4519

Molchan OV, Sokolovsky SG and Volotovsky ID. **The phytochrome control of the cAMP endogenous level in oat seedlings.** *Russian Journal of Plant Physiology* 2000, **47**: 463–467

Moutinho A, Hussey PJ, Trewavas AJ and Malho R. **cAMP acts as a second messenger in pollen tube growth and reorientation.** *Proceedings of the National Academy of Science* 2001, **98**:10481-10486.

Nabaneeta P, Curtin BF, Compton JR, Gordon RK and Nambiar MP. **Forskolin, an inducer of cAMP, up-regulates acetylcholinesterase expression and protects against organophosphate**

exposure in cells. Paper presented at the *Scientific Conference on Chemical and Biological Defense Research* 2004, Maryland, USA.

Nathanson JA. **Cyclic nucleotides and nervous system function.** *Physiological Research* **57**: 157-256

Nicholson D, White TD and Sawynok J. **Forskolin and phosphodiesterase inhibitors release adenosine but inhibit morphine-evoked release of adenosine from spinal cord synpatosomes.** *Canadian Journal of Physiology and Pharmacology* 1991, **69**(6): 877-885

Okamura N, Onoe S, Kawakura K, Tajima Y and Sugita Y. **Effects of membrane-bound trypsin-like proteinase and seminal proteinase inhibitors on the bicarbonate sensitive adenylate cyclase in porcine sperm plasma membranes.** *Biochimica et Biophysica Acta* 1990, **1035**(1): 83-89

Pan Q, Wendel J and Fluhr R. **Divergent evolution of plant NBS-LRR resistance gene homologues in dicot and cereal genomes.** *Journal of Molecular Evolution* 2000, **50**: 203-213

Psi-pred 2.5. **Protein Structure Prediction Server.** 2012. MEMSAT SVM PREDICTION. University College London Available at http://bioinf.cs.ucl.ac.uk/psipred/result/418422 on 07/06/12 at 1259hrs

Qi Z, Verma R, Gehring C, Yamaguchi Y, Zhao Y, Ryan CA and Berkowitz GA. **Ca^{2+} signaling by plant *Arabidopsis thaliana* Pep peptides depends on AtPepR1, a receptor with guanylyl cyclase activity, and cGMP-activated Ca^{2+} channels.** *Proceedings of the National Academy of Science* 2010, **107**(49): 21193-21198

Que YX, Xu LP, Lin JW and Chen RK. **Isolation and characterisation of NBS-LRR resistance gene analogs from sugarcane.** *Acta Agronomica Sinica* 2009, **35**(4): 631-639

Qutob D, Kemmerking B, Brunner F *et al*. **Phytotoxicity and innate immune responses induced by Nep1-like proteins.** *The Plant Cell* 2006, **18**(12): 3721-3744

Radwan O, Gandhi S, Heesacker A, Whitaker B, Taylor C, Plocik A, Kesseli R, Kozik A, Michel RW and Knapp SJ. **Genetic diversity and genomic distribution of hoologs encoding nbs-LRR disease resistance proteins in sunflower**. *Molecular Genetics and Genomics* 2008, **280**: 111-125

Rairdan G and Moffett P. **Brothers in arms?Common and contrasting themes in pathogen perception by plant NB-LRR and animal NACHT-LRR proteins.** *Microbes and Infection* 2007, **9**: 677-686

Recombinant Protein Solubility Prediction. University of Oklahoma. Available at http://www.biotech.ou.edu/ on 14/03/2012 at 1019hrs

Romeis T, Ludwig AA, Martin R and Jones JDG. **Calcium-dependent protein kinases play an essential role in a plant defence response.** *EMBO Journal* 2001, **20**: 5556–5567

Roshchina VV and Roshchina VD. **Ozone and the plant cell.** 2003. Kluwer Academic Publishers, Dordrecht, The Netherlands. pp 46-47

Rothberg JM, Jacobs JR, Goodman CS and Artavanis-Tsakonas S**. slit: an extracellular protein necessary for development of midline glia and commissural axon pathways contains both EGF and LRR domains.** *Genes Developments* 1990, **4**:2169-2187

Sadras V and Calderini. **Crop Physiology: Applications for Genetic Improvement and Agronomy.** 2009**,** Chapter 17, pp428 Academic Press.

Saijo Y, Hata S, Kyozuka J, Shimamoto K and Izui K**. Over-expression of a single Ca^{2+}-dependent protein kinase confers both cold and salt/drought tolerance on rice plants.** *The Plant Journal* 2000, **23**: 319–327

Seamon KB and Daly JW. **Forskolin: a unique dipertene activator of cyclic AMP-generating systems.** *Journal of Cyclic Nucleotide Research* 1981, **7**(4): 201-224

Seamon KB, Padgett W and Daly JW. **Forskolin: Unique diterpene activator of adenylate cyclase in membranes and in intact cells**. *Proceedings of the National Academy of Science* 1981, **78**(6): 3363-3367//

Stevens RC. **Design of high-throughput methods of protein production for structural biology.** *Structure* 2000, **8**: R177-R185

Suzuki N, Choe HR, Nishida Y, Yamawaki-Kataoka Y, Ohnishi S, Tamaoki T and Kataoka T. **Leucine-rich repeats and carboxyl terminus are required for interaction of yeast adenylate**

cyclase with RAS proteins. *Proceedings of the National Academy of Sciences* 1990, **87**(22): 8711-8715

Swiderski MR, Birker D and Jones JDG. **The TIR domain of TIR-NB-LRR resistance proteins is a signaling domain involved in cell death induction**. *Molecular Plant Microbe Interactions* 2009, **22**(2): 157-165

TAIR. **About Arabidopsis.** 2012. Available at http://www.arabidopsis.org/portals/education/aboutarabidopsis.jsp on 19/07/2012 at 1316hrs

Talke IN, Blaudez D, Maathuis FJM and Sanders D. **CNGCs: Prime targets of plant cyclic nucleotide signalling?** *Trends in Plant Science* 2003, **8**(6): 286–293

Tameling WIL and Joosten MHAJ. **The diverse roles of NB-LRR proteins in plants.** *Physiological and Molecular Plant Pathology* 2007, **71**: 126-134

Tang WJ and Gilman AG. **Construction of a soluble adenylyl cyclase activated by Gs alpha and forskolin.** *Science* 1995, **268**(5218): 1769-1772

Tarr DEK and Alexander HM**. TIR-NBS-LRR genes are rare in monocots: evidence from diverse monocot orders**. *BMC Research Notes* 2009, **2**:197-206

Tor M, Lotze MT and Holton N. **Receptor-mediated signaling in plants: molecular patterns and programmes.** *Journal of Experimental Botany* 2009, **60**(13): 3645-3654

Van der Hoorn RAL and Kamoun S. **From guard to decoy: A new model for perception of plant pathogen effectors**. *The Plant Cell* 2008, **20**: 2009-2017

Vidhyasekaran P. **Fungal pathogenesis in plants and crops: molecular biology and host defense mechanisms**. Volume 58. 2007. CRC.

Visconti PE, Muschietti JP, Flawia MM and Tezon JG. **Bicarbonate dependence of cAMP accumulation induced by phorbol esters in hamster spermatozoa**. *Molecular Cell Research* 1990, **1054**(2): 231-236

Wilczynski G, Kulma A, Sikorski AF and Szopa J. **ADP-ribosylation factor (ARF) regulates cAMP synthesis in potato.** *Journal of Plant Physiology* 1997, **151**(6): 689-698

Xiao S, Wang W and Yang X. **Evolution of resistance genes in plants.** Chapter 1. Innate immunity of plants, animals and humans. Heine H (Ed*). Nucleic Acids and Molecular Biology* 2008, pp 1-8. Springer-Verlag. Berlin ,Germany.

Zaccolo M, Cesetti T, di Benedetto G, Mongillo M, Lissandron V, Terrin A and Zamparo I. **Imaging the cAMP-dependent signal transduction pathway.** *Biochemical Society Transactions* 2005, **33**: 1323-1326

Zeilig CE, Johnson RA, Sutherland EW and Friedman DL. **Adenosine 3′:5′-monophosphate content and actions in the division cycle of synchronized HeLa cells.** *Journal of Cell Biology* 1976, **71**(2): 515